Supplementary Information

C2c2 is a single-component programmable RNA-guided RNA-targeting CRISPR effector

Omar O. Abudayyeh*[1,2,3,4], Jonathan S. Gootenberg[2,3,4,5]*, Silvana Konermann[2,3,4]*, Julia Joung[2,3,4], Ian M. Slaymaker[2,3,4], David B.T. Cox[1,2,3,4,6], Sergey Shmakov[7,8], Kira S. Makarova[8], Ekaterina Semenova[9], Leonid Minakhin[9], Konstantin Severinov[7,9,10], Aviv Regev[2,6], Eric S. Lander[2,5,6], Eugene V. Koonin[8,†], and Feng Zhang[1,2,3,4,†]

[1] Department of Health Sciences and Technology, Massachusetts Institute of Technology, Cambridge, Massachusetts 02139, USA

[2] Broad Institute of MIT and Harvard, Cambridge, Massachusetts 02142, USA

[3] McGovern Institute for Brain Research at MIT, Cambridge, Massachusetts 02139, USA

[4] Departments of Brain and Cognitive Science and Biological Engineering, Massachusetts Institute of Technology, Cambridge, MA 02139, USA

[5] Department of Systems Biology, Harvard Medical School, Boston, MA 02115, USA

[6] Department of Biology, Massachusetts Institute of Technology, Cambridge, Massachusetts 02139, USA

[7] Skolkovo Institute of Science and Technology, Skolkovo, 143025, Russia.

[8] National Center for Biotechnology Information, National Library of Medicine, National Institutes of Health, Bethesda, MD 20894, USA

[9] Waksman Institute for Microbiology, Rutgers, The State University of New Jersey, Piscataway, NJ 08854, USA

[10] Institute of Molecular Genetics, Russian Academy of Sciences, Moscow, 123182, Russia

* These authors contributed equally to this work.

[†] Correspondence should be addressed to zhang@broadinstitute.org (F.Z.) and koonin@ncbi.nlm.nih.gov (E.V.K.)

SUPPLEMENTARY MATERIALS AND METHODS

Cloning of C2c2 locus and screening libraries for MS2 activity Screen

Genomic DNA from *Leptotrichia shahii DSM 19757* (ATCC, Manassas, VA) was extracted using the Blood & Cell Culture DNA Mini Kit (Qiagen, Hilden, Germany) and the C2c2 CRISPR locus was PCR amplified and cloned into a pACYC184 backbone with chloramphenicol resistance. For retargeting of the locus to MS2 phage or endogenous targets, the wild type spacers in the array were removed and replaced with a Eco31I landing site an additional spacer and a degenerate repeat, compatible with Golden Gate cloning.

A custom library consisting of all possible spacers targeting the genome of the bacteriophage MS2, excluding spacers containing the Eco31I restriction site, was synthesized by Twist Biosciences (San Francisco, CA), cloned into the retargeting backbone with Golden Gate cloning, transformed into Endura Duo electrocompetent cells (Lucigen, Middleton, WI) and subsequently purified using a NucleoBond Xtra MaxiPrep EF (Machery-Nagel, Düren, Germany).

Cloning of libraries and screening for β–lactamase and transcribed/non-transcribed PFS screens

Plasmid libraries for PFS screens were cloned from synthesized oligonucleotides (IDT, Coralville, IA) consisting of either 6 or 7 randomized nucleotides downstream of the spacer 1 target (completed plasmids in Table S5). To generate dsDNA fragments for cloning, these ssDNA oligonucleotides were annealed to a short primer for second strand synthesis by large Klenow fragment (New England Biolabs, Ipswich, MA). dsDNA fragments were Gibson cloned (New England Biolabs) into digested pUC19 at the 5'-region of β–lactamase, downstream of the lac promoter, or in a non-transcribed region of pUC19 and electroporated into Endura Duo electrocompetent cells (Lucigen). More than $5*10^6$ cells were collected, pooled, and harvested for plasmid DNA using a NucleoBond Xtra MaxiPrep EF (Machery-Nagel, Düren, Germany). To screen libraries, we co-transformed 50 ng of the pooled library and an equimolar amount of the LshC2c2 locus plasmid or pACYC184 plasmid control into *E. coli* cells (NovaBlue

GigaSingles, EMD Millipore, Darmstadt, Germany). After transformation, cells were plated on ampicillin and chloramphenicol to select for both plasmids. After 16 hours of growth, $>1*10^6$ cells were harvested for plasmid DNA using a NucleoBond Xtra MaxiPrep EF (Machery-Nagel) The target PFS region was PCR amplified and sequenced using a MiSeq (Illumina, San Diego, CA) with a single-end 150 cycle kit.

Bacterial phage interference PFS screen assay

For the phage screen, 50ng of the plasmid library were transformed into NovaBlue(DE3) Competent Cells (EMD Millipore) followed by an outgrowth at 37°C for 30 minutes. Three different replicates of cells were then grown in Luria broth (LB, Miller's modification, 10g/L tryptone, 5g/L yeast extract, 5g/L NaCl, Sigma, St. Louis, MO) supplemented with 25 μg/mL chloramphenicol (Sigma) in a volume of 3.0mL for 30 minutes. Phage conditions were treated with $7*10^9$ (10^{-1} dilution), $7*10^7$ (10^{-3} dilution), or $7*10^5$ (10^{-5} dilution) PFU of Bacteriophage MS2 (ATCC). After 3 hours of shaking incubation at 37°C, samples were plated on LB-agar plates supplemented with chloramphenicol and harvested after 16 hours. DNA was extracted using NucleoBond Xtra MaxiPrep EF (Machery-Nagel), PCR amplified around the guide region, and sequenced using a MiSeq (Illumina) with a paired-end 150 cycle kit.

Bacterial phage interference assay for individual spacers

To test individual spacers for MS2 interference, the oligonucleotides encoding the spacer sequences (Table S4) flanked by Eco31I sites were ordered from IDT as complementary strands. The oligonucleotides (final concentration 10μM) were annealed in 10X T4 ligase buffer (New England Biolabs; final concentration 1X) supplemented with 5 units of T4 PNK (New England Biolabs). The oligonucleotides were phosphorylated by setting the thermocycler to 37°C for 30 minutes and then subsequently annealed by heating to 95°C for 5 minutes followed by a -5°C/minute ramp down to 25°C. Annealed oligos were then cloned into the locus backbone with Golden Gate cloning. Plasmids were transformed into C3000 strain *E. coli,* and the cultures were made competent with the Mix and Go kit (Zymo Research, Irvine, CA). C3000 cells were seeded from an overnight culture grown to OD_{600} of 2, at which point they were diluted 1:13 in Top Agar (10g/L tryptone, 5g/L yeast extract, 10g/L NaCl, 7g/L agar) and poured on LB-chloramphenicol plates. Dilutions of MS2 phage in phosphate buffered saline were then spotted

on the plates using a multichannel pipette, and plaque formation was recorded after overnight incubation.

RFP targeting assay

An ampicillin resistant RFP-expressing plasmid (pRFP) was transformed into DH5-alpha cells (New England Biolabs). Cells containing pRFP were then made chemically competent (Mix and Go, Zymo Research) to be used for downstream targeting experiments with pLshC2c2. Spacers targeting RFP mRNA were cloned into pLshC2c2 (as described above) and these plasmids were transformed into the chemically competent DH5-alpha pRFP cells. Cells were then grown overnight under double selection in LB and subjected to analysis by flow cytometry when they reached an OD600 of 4.0. Knockdown efficiency was quantified as the percent of RFP positive cells compared to a non-targeting spacer control (the endogenous LshC2c2 locus in pACYC184).

To interrogate the effect of LshC2c2 activity on the growth of the host cells, we created a TetR-inducible version of the RFP plasmid in pBR322 (pBR322_RFP). We transformed *E. coli* cells with this vector and then made them chemically competent (Mix and Go, Zymo Research) to prepare them for downstream experiments. We cloned pLshC2c2 plasmids with various spacers targeting RFP mRNA as well as their reverse complement controls and transformed them into *E. coli* cells carrying pBR322_RFP and streaked them on double-selection plates to maintain both plasmids. Colonies were then picked and grown overnight in LB with double selection. Bacteria were diluted to an OD_{600} of 0.1 and grown at 37C for 1 hour with chloramphenicol selection only. RFP expression was then induced using dilutions of anhydrotetracycline (Sigma) and OD_{600} measurements were taken every 6 minutes under continuous shaking in a Synergy 2 microplate reader (BioTek, Winooski, VT).

C2c2 protein purification

The mammalian codon-optimized gene for C2c2 (*Leptotrichia shahii)* was synthesized (GenScript, Jiangsu, China) and inserted into a bacterial expression vector (6-His-MBP-TEV, a pET based vector generously provided by Doug Daniels) using Golden Gate cloning. The LshC2c2 expression construct was transformed into One Shot® BL21(DE3)pLysE (Invitrogen, Carlsbad, CA) cells. 10mL of overnight culture were inoculated into 12 liters of Terrific Broth

growth media (12g/L tryptone, 24g/L yeast extract, 9.4g/L K_2HPO, 2.2g/L KH_2PO_4, Sigma) supplemented with 100 μg/mL. Cells were then grown at 37 °C to a cell density of 0.2 OD_{600}, at which point the temperature was lowered to 21°C. At a cell density of 0.6 OD_{600}, MBP-LshC2c2 expression was induced by supplementing with IPTG to a final concentration of 500 μM. Induced culture was grown for 14-18 hours before harvesting cell paste, which was stored at -80°C until subsequent purification.

Frozen cell paste was crushed and resuspended via stirring at 4°C in 1L of Lysis Buffer (50 mM Hepes pH 7, 2M NaCl, 5 mM $MgCl_2$, 20 mM imidazole) supplemented with protease inhibitors (cOmplete, EDTA-free, Roche Diagnostics Corporation, Indianapolis, IN). The resuspended cell paste was lysed by lysozyme (Sigma) addition and sonication (Sonifier 450, Branson, Danbury, CT). Lysate was cleared by centrifugation at 10,000g for 1 hour, and the supernatant was filtered through Stericup 0.45 micron filters (EMD Millipore). Filtered lysate was incubated with Ni-NTA superflow nickel resin (Qiagen) at 4°C for 1 hour with gentle agitation, and then applied to an Econo-column chromatography column (Bio-Rad Laboratories, Hercules, CA). Resin was washed with lysis Buffer and eluted with a gradient of imidazole. Fractions containing protein of the expected size for MBP-LshC2c2 were pooled and buffer exchanged into TEV Buffer (500 mM NaCl, 50 mM Hepes pH 7, 5 mM MgCl, 2 mM DTT) with Ultra-15 Centrifugal Filter Unit with 50 KDa cutoff (Amicon, EMD Millipore). TEV protease (Sigma) was added and incubated at 4°C overnight. After incubation, TEV cleavage was confirmed by SDS-PAGE and Coomassie staining, and the sample was concentrated via Centrifugal Filter Unit to 1 mL. Concentrated sample was loaded a gel filtration column (HiLoad 16/600 Superdex 200, GE Healthcare Life Sciences, Chalfont Saint Giles, United Kingdom) via FPLC (AKTA Pure, GE Healthcare Life Sciences). The resulting fractions from gel filtration were tested for presence of LshC2c2 protein by SDS-PAGE; fractions containing LshC2c2 were pooled, buffer exchanged into Storage Buffer (1 M NaCl, 50 mM Tris-HCl pH 7.5, 5% glycerol, 2 mM DTT), concentrated, and either used directly for biochemical assays or frozen at -80°C for storage. To calculate the approximate size of recombinant LshC2c2, gel filtration standards were run on the same gel filtration column equilibrated in 2M NaCl, Hepes pH 7.0.

C2c2 HEPN mutant protein purification

Alanine mutants at each of the four HEPN catalytic residues were generated by Gibson cloning and transformed into One Shot® BL21(DE3)pLysE cells (Invitrogen). For each mutant, 6 L of Terrific Broth were used to generate cell paste. Protein purification was performed similarly to wild type C2c2 with exception of buffer composition being altered to increase stability of recombinant protein in solution. Detergent or glycerol was added to Lysis Buffer (50 mM Hepes pH 7, 1M NaCl, 5 mM $MgCl_2$, 20 mM imidazole, 1% Triton X-100), Imidazole Elution Buffer Buffer (50 mM Hepes pH 7, 1M NaCl, 5 mM $MgCl_2$, 200 mM imidazole, 0.01% Triton X-100, 10% glycerol) and TEV Buffer (500 mM NaCl, 50 mM Hepes pH 7, 5 mM MgCl, 1 mM DTT, 0.01% Triton X-100, 10% glycerol). In all situations where HEPN mutants were used biochemical analysis, wild type protein used for comparison was purified in the same manner.

Nucleic acid target preparation

DNA oligo templates for T7 transcription were ordered from IDT (Tables S2, S3). Templates for crRNAs were annealed to a short T7 primer (final concentrations 10μM) and incubated with T7 polymerase overnight at 37°C using the HiScribe T7 Quick High Yield RNA Synthesis kit (New England Biolabs). Target templates were PCR amplified to yield dsDNA and then incubated with T7 polymerase at 30°C overnight using the same kit.

5' end labeling was accomplished using the 5' oligonucleotide kit (VectorLabs, Burlingame, CA) and with a maleimide-IR800 probe (LI-COR Biosciences, Lincoln, NE). 3' end labeling was performed using a 3' oligonucleotide labeling kit (Sigma) using ddUTP-Cy5. Labeled probes were purified using Clean and Concentrator columns (Zymo Research).

dsRNA substrates were prepared by mixing 5'-end-labeled ssRNA targets with two-fold excess of non-labeled complementary ssRNA oligos in annealing buffer (30mM HEPES pH 7.4, 100 mM potassium acetate, and 2mM magnesium acetate). Annealing was performed by incubating the mixture for 1 minute at 95°C followed by a -1°C/minute ramp down to 23°C.

Nuclease Assay

Nuclease assays were performed with 160nM of end-labeled ssRNA target, 200nM purified LshC2c2, and 100nM crRNA, unless otherwise indicated, in nuclease assay buffer (40mM Tris-HCl, 60mM NaCl, 6mM MgCl2, pH 7.3). Reactions were allowed to proceed for 1 hour at 37°C (unless otherwise indicated) and were then quenched with proteinase buffer (proteinase K, 60mM EDTA, and 4M Urea) for 15 minutes at 37°C. The reactions were then denatured with 4.5M urea denaturing buffer at 95°C for 5 minutes. Samples were analyzed by denaturing gel electrophoresis on 10% PAGE TBE-Urea (Invitrogen) run at 45°C. Gels were imaged using an Odyssey scanner (LI-COR Biosciences).

Electrophoretic mobility shift assay

Target ssRNA binding experiments were performed with a series of half-log complex dilutions (crRNA and LshC2c2) from 2μM to 0.2pM (or 1μM to 0.1pM in the case of R1278A LshC2c2). Binding assays were performed in nuclease assay buffer supplemented with 10mM EDTA to prevent cutting, 5% glycerol, and 10μg/mL heparin in order to avoid non-specific interactions of the complex with target RNA. Reactions were incubated at 37°C for 20 minutes and then resolved on 6% PAGE TBE gels (Invitrogen) at 4°C (using 0.5X TBE buffer). Gels were imaged using an Odyssey scanner (LI-COR Biosciences).

Next-generation sequencing of *in vitro* cleaved RNA

In vitro nuclease assays were performed as described above using unlabeled ssRNA targets. After one hour, samples were quenched with proteinase K + EDTA and then column purified (Clean and Concentrator, Zymo Research). The RNA samples were PNK treated in absence and presence of ATP to allow for the enrichment of 3'-P and 5'-OH ends, respectively. The samples were then polyphosphatase treated (Epicentre, Madison, WI) before being prepared for next-generation sequencing using the NEBNext Small RNA Library Prep Set for Illumina sequencing (New England Biolabs) with the PCR extension step increased to allow for longer templates to be included in the library. Libraries were sequenced on an MiSeq (Illumina) to sufficient depth and analyzed using the alignment tool BWA (*53*). Paired-end alignments were used to extract entire transcript sequences using Galaxy tools (https://usegalaxy.org/), and these sequences were

analyzed using Geneious 8.1.5 (Biomatters, Auckland, New Zealand) and custom scripts (github.com/fengzhanglab).

In vitro co-transcriptional DNA cleavage assay

The *E. coli* RNAP co-transcriptional DNA cleavage assay was performed essentially as described previously (*22*). Briefly, 0.8pmol of ssDNA template strand were annealed with 1.6pmol of RNA in transcription buffer (from *E. coli* RNAP core enzyme, New England Biolabs) without magnesium to prevent RNA hydrolysis. 0.75ul of *E. coli* RNAP core enzyme and Magnesium were added and the reaction incubated at 25°C for 30min and then transferred to 37°C. 1pmol of freshly denatured nontemplate strand (NTS) were added and incubated at 37°C for 15min to obtain elongation complexes (ECs). 4pmol of LshC2C2-crRNA complexes along with 1.25 mM of RNTPs were added to the ECs and transcription was allowed to proceed for 1h at 37°C. DNA was resolved by denaturing gel electrophoresis on a 10% PAGE TBE-Urea (Invitrogen) gels following RNase and proteinase K treatment.

Computational analysis of *in vivo* PFS screens

To determine enriched spacers in the bacterial phage interference screens, spacer regions were extracted, counted, and normalized to total reads for each sample. For a given spacer, enrichment was measured as the $\log_2$ ratio compared to the no phage conditions, with a 1.0 psuedocount adjustment. 5' and 3' PFS regions from spacers above a 1.25 $\log_2$ enrichment threshold that occurred in all three biological replicates were used to generate sequence logos for the phage dilution samples (*54*). Correlations between replicate conditions were measured using a Kendall's Tau rank correlation and the information coefficient, a mutual information based metric for ascertaining similarity (*43, 55*).

For the β-lactamase PFS screen and transcribed/non-transcribed pUC19 PFS screens, PFS regions were extracted, computationally collapsed to 5nt to increase coverage, counted, and normalized to total reads for each sample. For a given PFS, enrichment was measured as the log ratio compared to pACYC184 control, with a 0.01 psuedocount adjustment. PFSs above a 6 depletion threshold (β-lactamase screen), a 0.35 depletion threshold (transcribed pUC19 screen),

or a 0.5 depletion threshold (non-transcribed pUC19 screen) that occurred in both biological replicates were collected and used to generate sequence logos (*54*).

SUPPLEMENTARY FIGURES

Figure S1

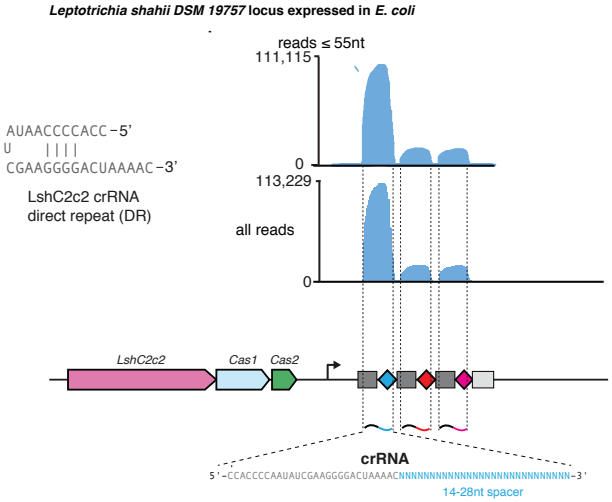

Fig. S1: RNA-sequencing of the *Leptotrichia shahii* locus heterologously expressed in *E. coli* and spacer analysis. Adapted from (*19*).

Heterologous expression of the LshC2c2 locus reveals processing of the array. Insert: *In silico* co-folding analysis of a mature direct repeat.

Figure S2

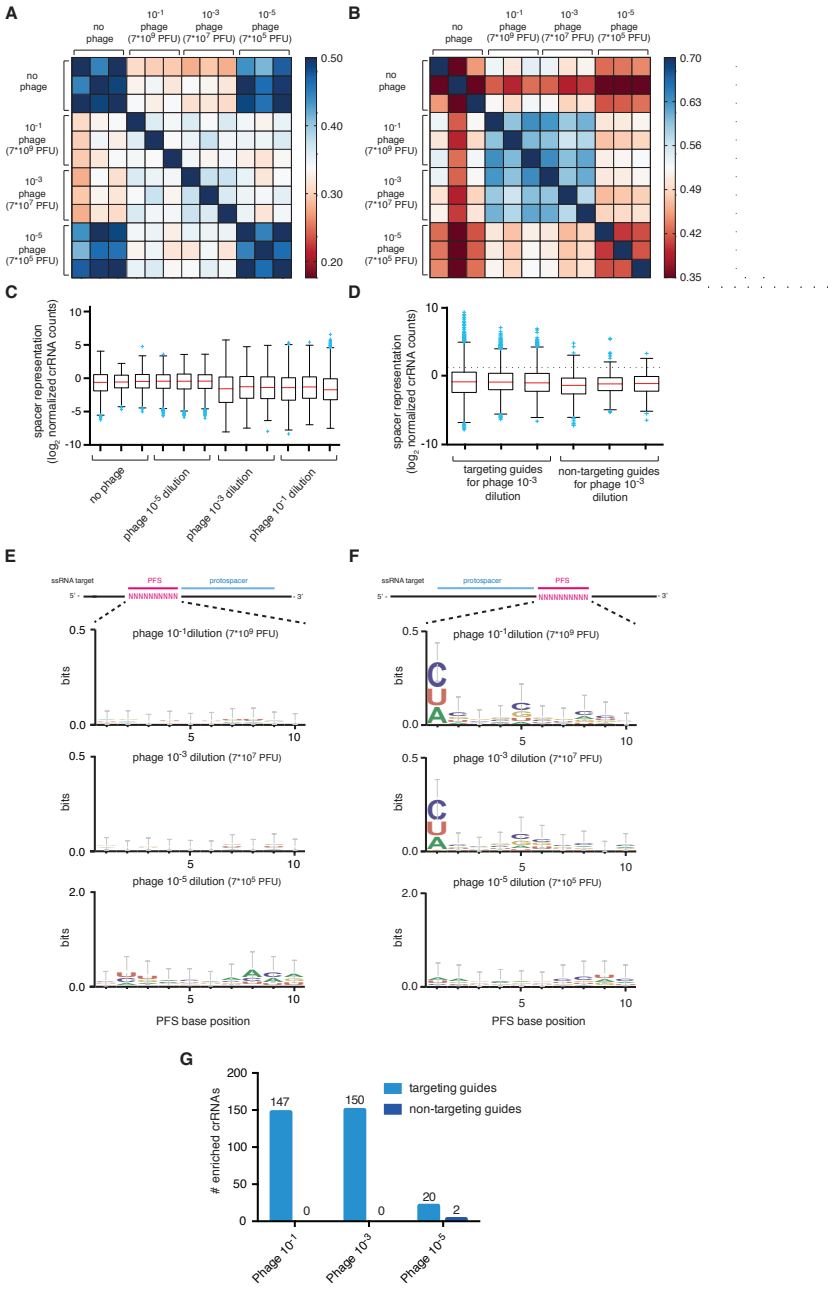

Fig. S2: MS2 phage screen replicates show agreement and do not have a 5' PFS

(A) Rank correlation (Kendall) of normalized crRNA count distributions between replicate conditions in the screen. (B) Information coefficient representing the mutual information between the normalized crRNA count distributions of replicate conditions in the screen. This metric highlights how similar the 10^{-1} and 10^{-3} dilution conditions are and how little information

is shared between 10^{-1}/10^{-3} and 10^{-5}/no phage groups. A higher information coefficient represents strong correlation and is computed as previously described (*43, 55*). (C) Box plot showing the distribution of normalized crRNA frequencies for the phage-treated conditions (10^{-1}, 10^{-3}, and 10^{-5} dilutions) and control screen (no phage) biological replicates (n = 3). The box extends from the first to third quartile with whiskers denoting 1.5 times the interquartile range. The mean is indicated by the red horizontal bar. The 10^{-1} and 10^{-3} phage dilution distributions are significantly different than each of the control replicates (****, $p < 0.0001$). (C) Box plot showing the distribution of normalized crRNA frequencies (normalized to no phage condition) for targeting and non-targeting guides from the 10^{-3} diluted phage conditions (n=3). (D) (E) Sequence logo of 5' sequences from enriched spacers in each of the phage dilutions. (F) Sequence logos of 3' sequences from enriched spacers in the 10^{-1} and 10^{-3} phage dilutions show a PFS. (G) The number of targeting and non-targeting control spacers that are consistently enriched (the exact number is above each bar). A spacer is considered enriched only if it has a $\log_2$ normalized crRNA fold change > 1.25 in all three replicates. Within the consistently enriched crRNAs, there are 84 sequences that are shared between the 10^{-1} and 10^{-3} conditions.

Figure S3

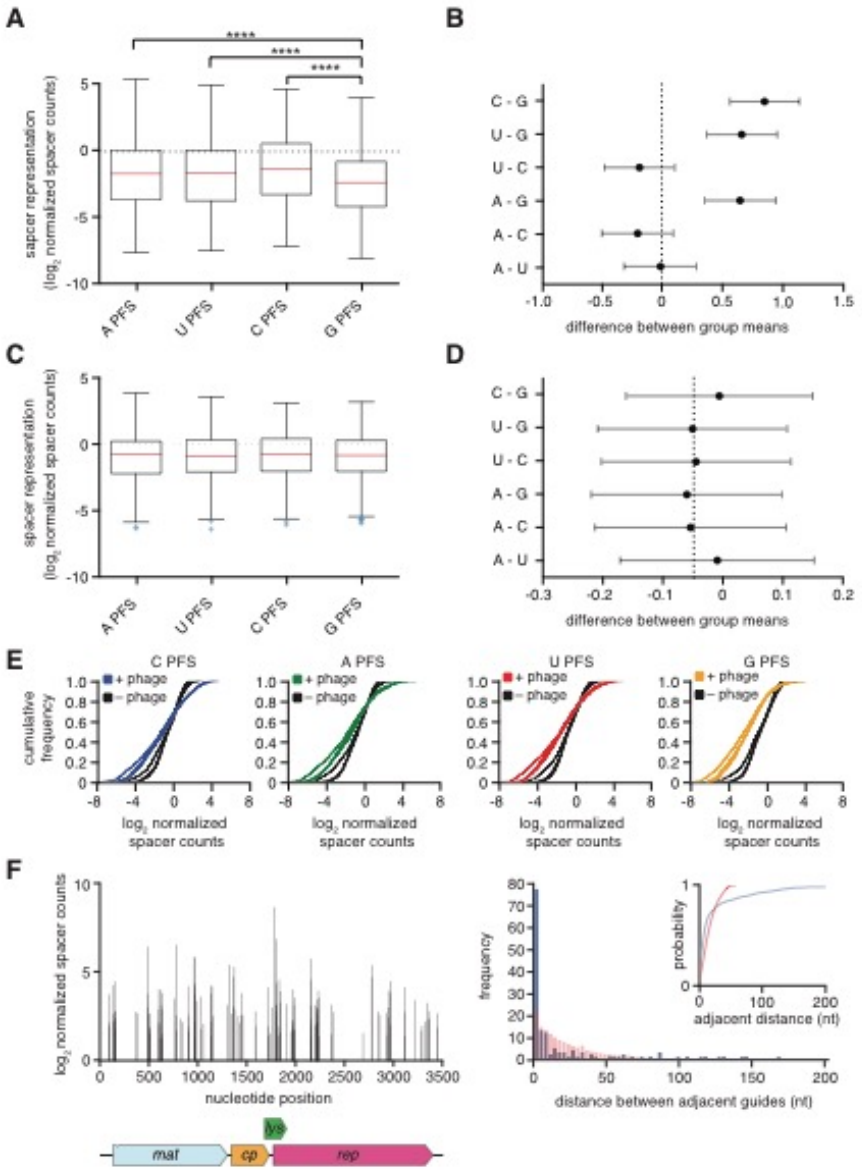

Fig. S3: MS2 phage screen spacer representation across each PFS.

(A) Box plot showing the distribution of spacer frequencies with spacers grouped by their 3' PFS for 10^{-3} phage treated conditions. Box extends from the first to third quartile with the whiskers denoting 1.5 times the interquartile range. ****, $p < 0.0001$. (B) Multiple comparison test (ANOVA with Tukey correction) between all possible PFS pairs for the 10^{-3} phage treated spacer distributions. Plotted are the 95% confidence intervals for difference in means between the

compared PFS pairs. (C) Box plot showing the distribution of spacer frequencies with spacers grouped by their 3' PFS for non-phage treated conditions. Box extends from the first to third quartile with the whiskers denoting 1.5 times the interquartile range. (D) Multiple comparison test (ANOVA with Tukey correction) between all possible PFS pairs for the non-phage treated spacer distributions. Plotted are the 95% confidence intervals for difference in means between the compared PFS pairs. (E) Cumulative frequency plots for the $\log_2$ normalized spacer counts. Spacers are separated by respective PFS to show the enrichment differences between the 10^{-3} phage and control PFS distributions. (F) The enriched spacers from the 10^{-3} dilution condition are plotted according to their position along the MS2 genome. The corresponding gene positions are mapped below. (G) Frequency distributions of the non-redundant nearest-neighbor pairwise-distances between all 150 enriched guides in the 10^{-3} phage dilution condition (blue) and in a bootstrapped simulation of 150 randomly chosen guides (n=10,000) (red). A significant difference between both distributions is observed using a two-sample Kolmogorov-Smirnov statistic (****, $p < 0.0001$). Inset: the cumulative frequency distributions for the non-redundant nearest-neighbor pairwise-distance distributions for the 10^{-3} phage dilution condition (blue) and bootstrapped simulation (red).

Figure S4

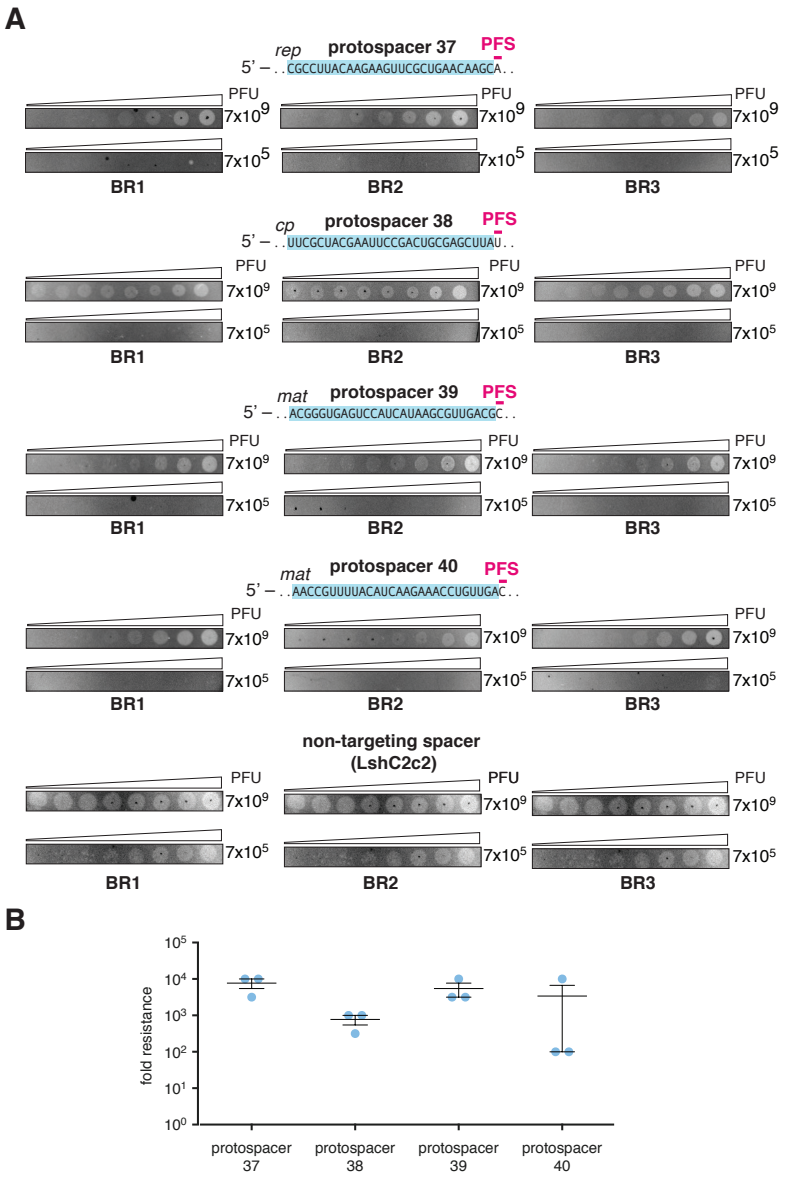

Fig. S4: Top hits from MS2 phage screen show interference in plaque assay

(A) Images from validation of MS2 screen by plaque assay showing reduced plaque formation in top hits. Phage dilutions were spotted on bacteria plates at decreasing numbers of plaque forming units (PFU). Spacer targets are shown above images; biological replicates are labeled BR1, BR2, or BR3. Non-targeting control is the native LshC2c2 locus. (B) Quantitation of MS2 plaque assay demonstrating interference by top hits. Interference was quantified by highest dilution without plaques. Bars plotted are the mean ± s.e.m.

Figure S5

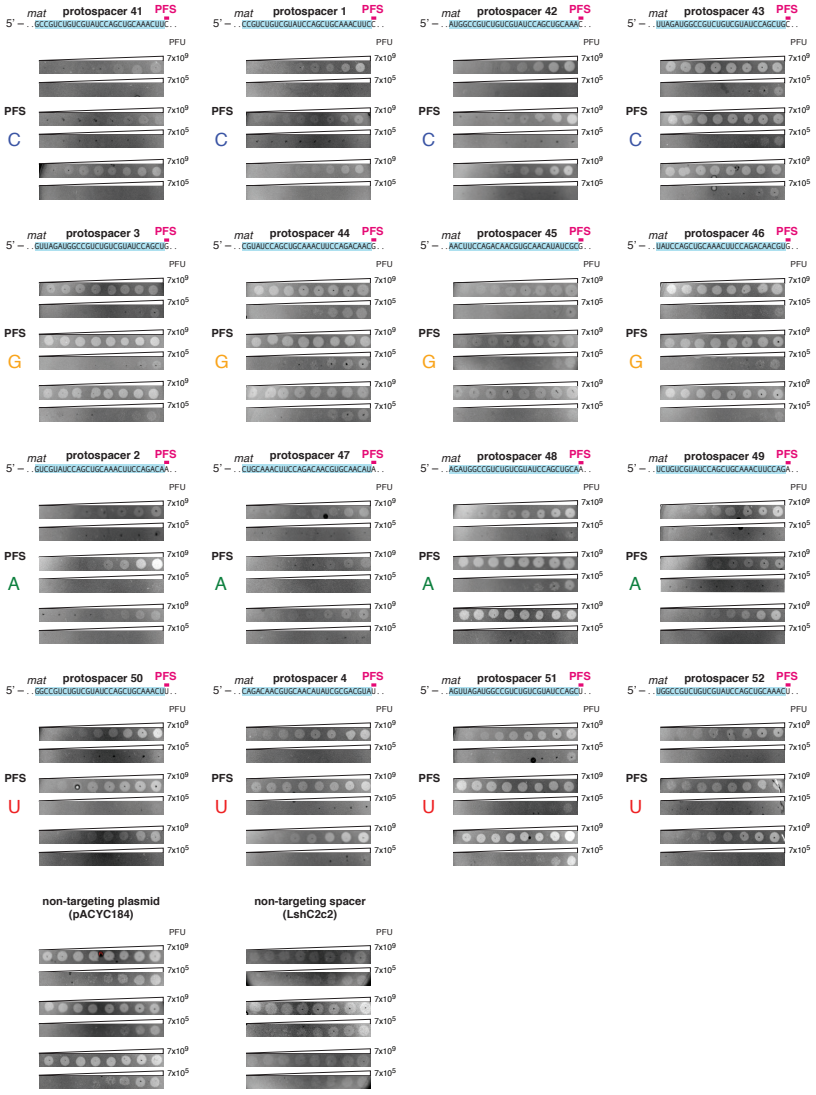

Fig. S5: MS2 plaque assay validates the 3' H PFS.

Four spacers for each possible 3' PFS (A, G, C, and U) are cloned into the pLshC2c2 vector and tested for MS2 phage restriction in a plaque forming assay. The images show significantly reduced plaque formation for A, C, and U PFSs, and less restriction for the G PFS. Phage dilutions were spotted on bacteria plates at decreasing numbers of plaque forming units (PFU). Spacer targets are shown above images; three biological replicates are vertically stacked under

each protospacer sequence. Non-targeting controls are the native LshC2c2 locus and the pACYC184 backbone.

Figure S6

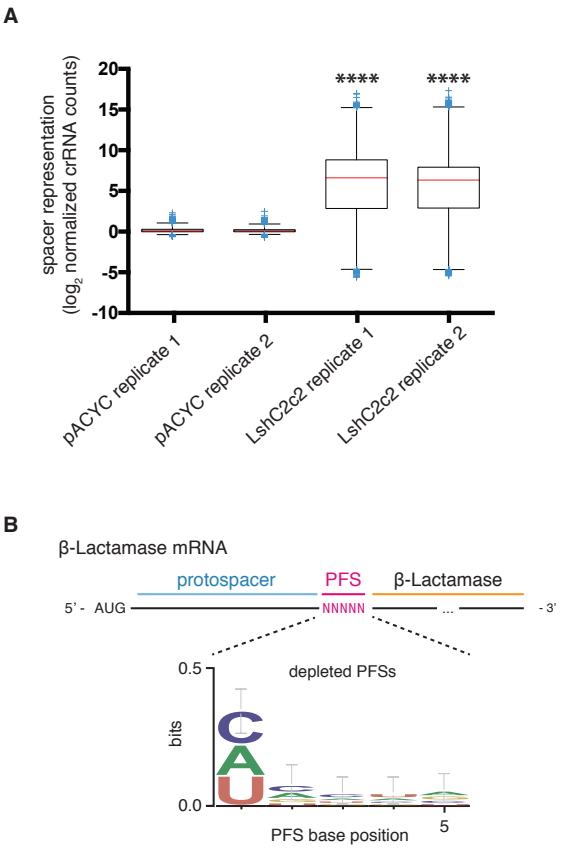

Fig. S6. A PFS screen in the β-lactamase mRNA reveals a 3' H PFS

(A) Comparison of the normalized crRNA count distributions for the pACYC control and LshC2c2 replicates (n=2). Box plots are shown with boxes extending from the first quartile to third quartile and whiskers denoting 1.5 times the interquartile range. Significant enrichment and depletion is observed in the LshC2c2 replicates (****, $p < 0.0001$). (B) A 3' PFS is observed from the depleted PFSs ($-\log_2$ normalized PFS count fold change >6.0).

Figure S7

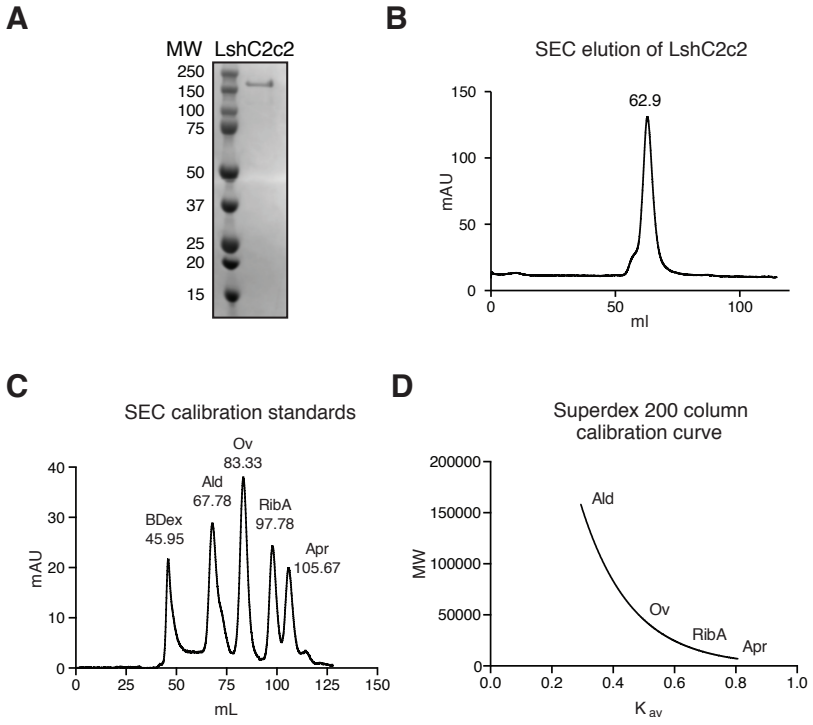

Fig. S7: Protein purification of LshC2c2.

(A) Coomassie blue stained acrylamide gel of purified LshC2c2 stepwise purification. A strong band just above 150 kD is consistent with the size of LshC2c2 (171 kD). (B) Size exclusion gel filtration of LshC2c2. LshC2c2 eluted at a size approximately >160 kD (62.9 mL). (C) Protein standards used to calibrate the Superdex 200 column. BDex = Blue Dextran (void volume), Ald = Aldolase (158 kD), Ov = Ovalbumin (44 kD), RibA = Ribonuclease A (13.7 kD), Apr = Aprotinin (6.5 kD). (D) Calibration curve of the Superdex 200 column. K_{av} is calculated as (elution volume – void volume)/(geometric column volume – void volume). Standards were plotted and fit to a logarithmic curve.

Figure S8

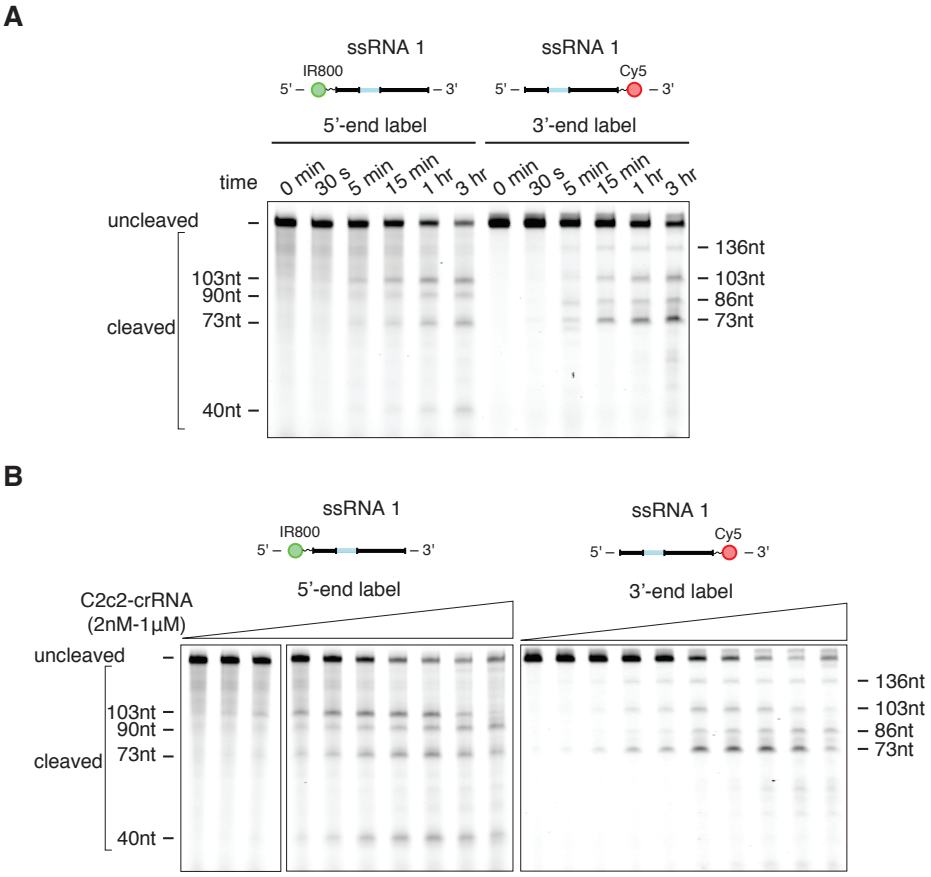

Fig. S8: Further *in vitro* characterization of the RNA cleavage kinetics of LshC2c2.

(A) Denutaring gel of a time series of LshC2c2 ssRNA cleavage using a 5'- and 3-end-labeled target 1. (B) A denaturing gel after 1 hour of RNA-cleavage of 5'- and 3-end-labeled target 1 using LshC2c2-crRNA complex that is serially diluted in half-log steps. Reported band lengths are matched from RNA sequencing.

Figure S9

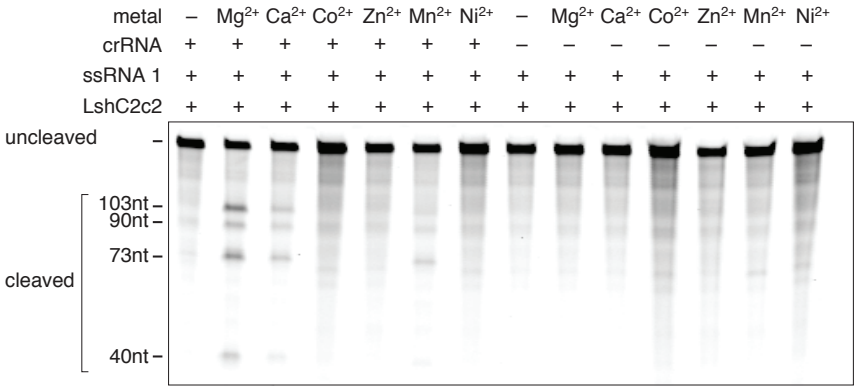

Fig. S9: Characterization of the metal dependence of LshC2c2 RNA cleavage.

A variety of divalent metal cations are supplemented for the LshC2c2 cleavage reaction using 5'-end-labeled target 1 incubated for 1 hour. Significant cleavage is only observed for Mg^{+2}. Weak cleavage is observed for Ca^{+2} and Mn^{+2}. Reported band lengths are matched from RNA sequencing.

Figure S10

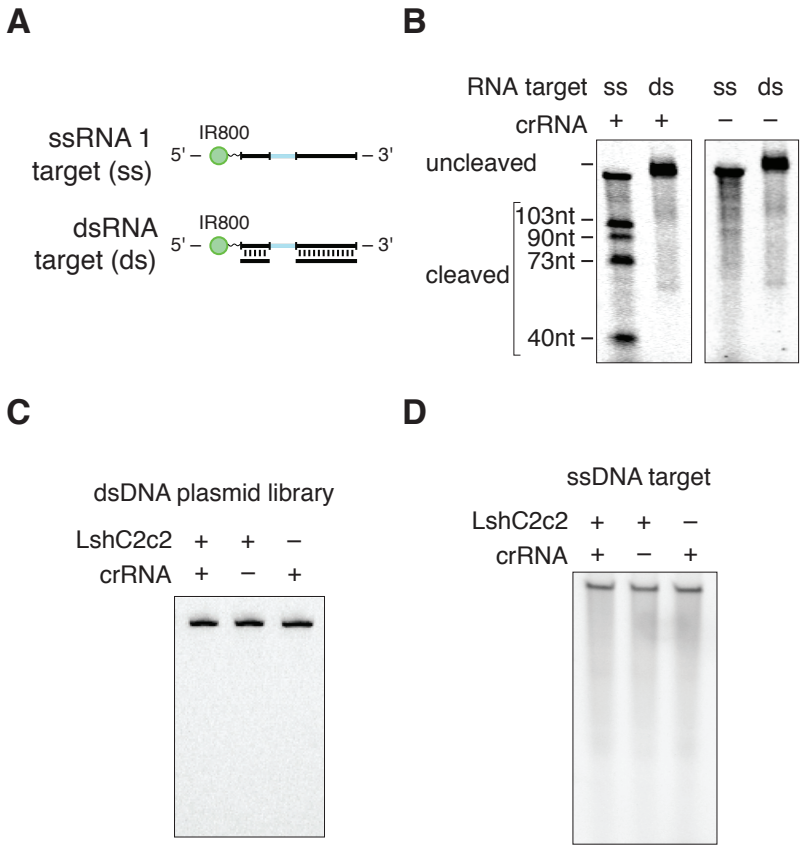

Fig. S10: LshC2c2 has no observable cleavage activity when using dsRNA, dsDNA, or ssDNA substrates.

(A) A schematic of the partial dsRNA target. 5'-end-labeled target 1 is annealed to two shorter RNAs that are complementary to the regions flanking the protospacer site. This partial dsRNA is a more stringent test for dsRNA cutting since it should still allow for LshC2c2 complex binding to ssRNA. (B) LshC2c2 cleavage activity after 1 hour of incubation with a dsRNA target shown in (A) compared to the ssRNA target 1. No cleavage is observed when using the dsRNA substrate. Reported band lengths are matched from RNA sequencing. (C) LshC2c2 cleavage of a dsDNA plasmid library incubated for 1 hour. A plasmid library was generated to have seven randomized nucleotides 5' of protospacer 14 to account for any sequence requirements for dsDNA cleavage. No cleavage is observed for this dsDNA library. (D) A ssDNA version of target 1 is tested for cleavage by LshC2c2 after 1 hour of incubation. No cleavage is observed.

Figure S11

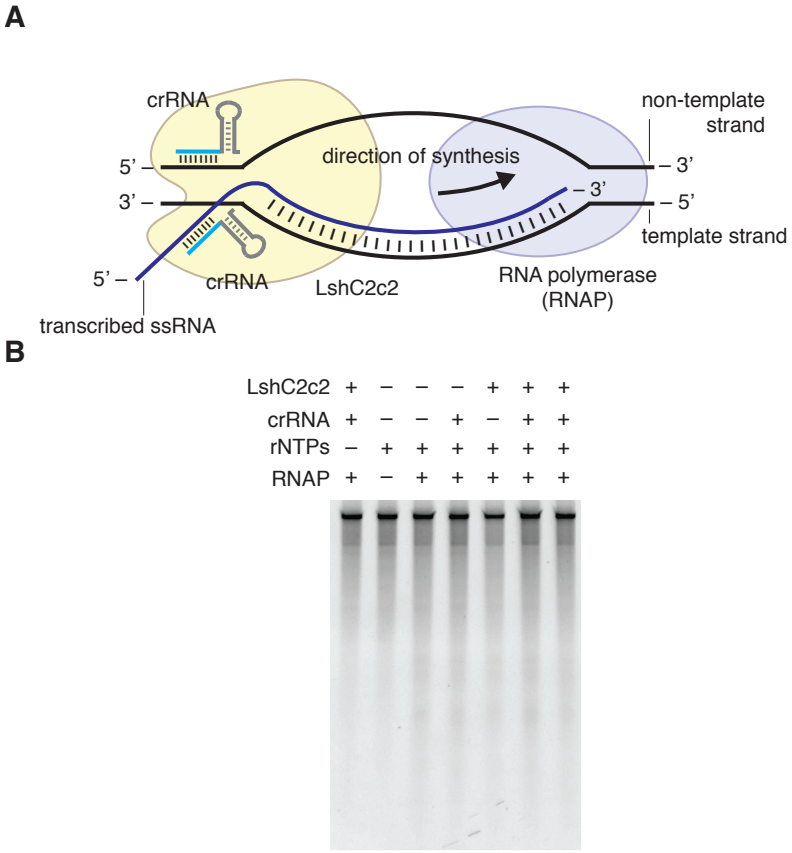

Fig. S11: LshC2c2 has no observable cleavage activity on dsDNA targets in a co-transcriptional cleavage assay

(A) Schematic of co-transcriptional cleavage assay. C2c2 was incubated with *E. coli* RNA polymerase (RNAP) elongation complexes and rNTP as previously described (*22*). (B) LshC2c2 cleavage of DNA target after co-transcriptional cleavage assay. No cleavage is observed.

Figure S12

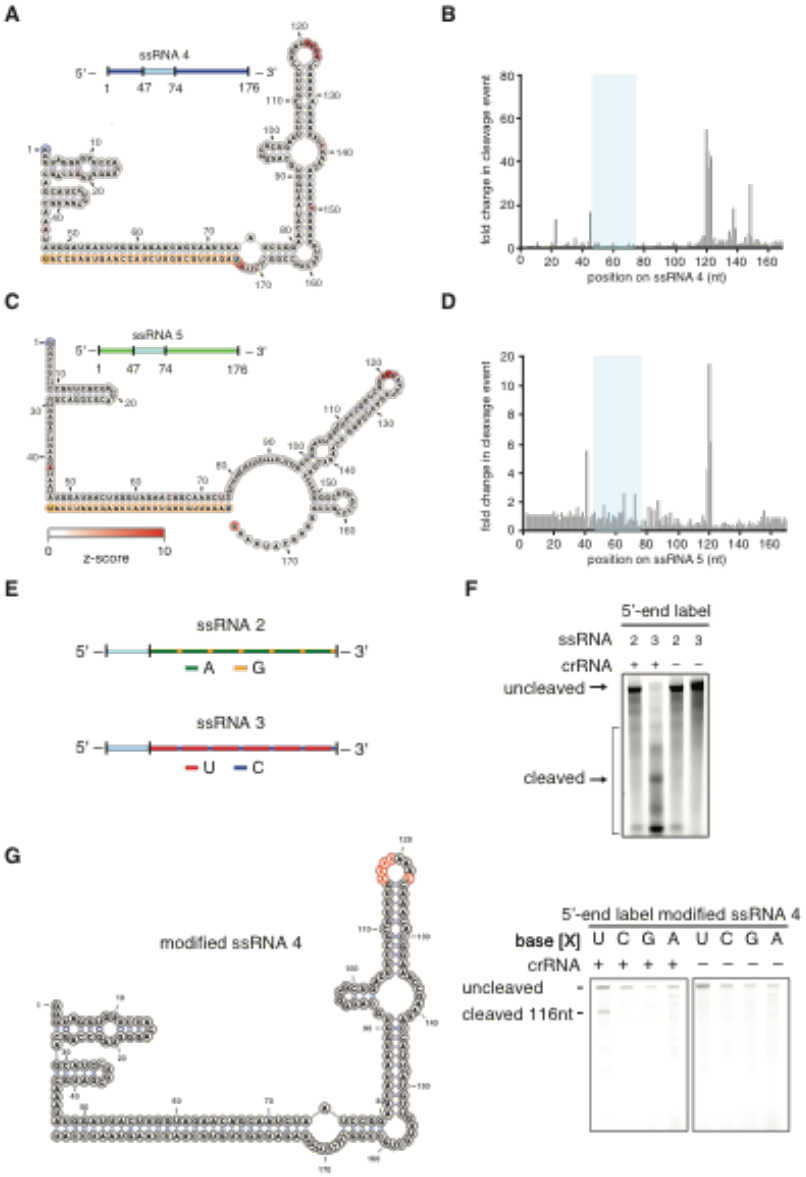

Fig. S12: Figure 4. LshC2c2 prefers cleavage at uracil residues.

(A,C) The cleavage sites of non-homopolymer ssRNA targets 4 (A), and 5 (C) were mapped with RNA-sequencing of the cleavage products. The frequency of cleavage at each base is colored according to the z-score and shown on the predicted crRNA-ssRNA co-fold secondary structure. Fragments used to generate the frequency analysis contained the complete 5' end. The

5’ and 3’ end of the ssRNA target are indicated by blue and red outlines, on the ssRNA and secondary structure, respectively. The 5’ and 3’ end of the spacer (outlined in yellow) is indicated by the blue and orange residues highlighted respectively. (B,D) Plot of the frequencies of cleavage sites for each position of ssRNA targets 4 and 5 for all reads that begin at the 5’ end. The protospacer is indicated by the blue highlighted region. (E) Schematic of homopolymer ssRNA targets. The protospacer is indicated by the light blue bar. Homopolymer stretches of A (green) and U (red) bases are interspaced by individual bases of G (orange) and C (purple). (F) Denaturing gel showing C2c2-crRNA-mediated cleavage patterns of each homopolymer after 3 hours of incubation. (G) Schematic of ssRNA 4 modified with a hompolymer stretch in the highlighted loop (red) for each of the four possible nucleotides (*left)*. Denaturing gel showing C2c2-crRNA-mediated cleavage for each of the four possible homopolymer targets after 3 hours of incubation. Reported band lengths are matched from RNA sequencing.

Figure S13

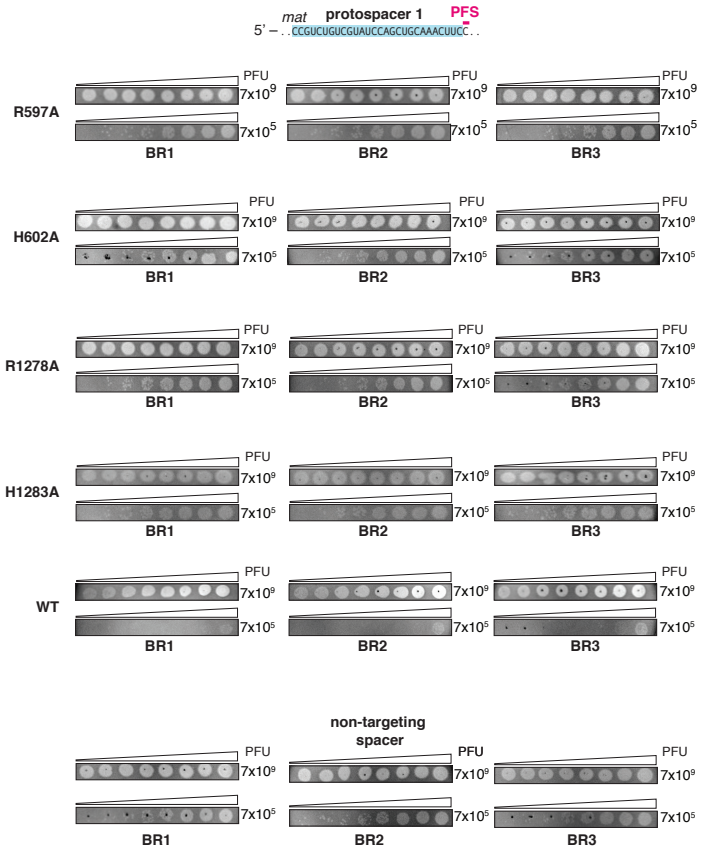

Fig. S13: MS2 restriction assay reveals that single HEPN mutants abrogate LshC2c2 activity.

All four possible single HEPN mutants were generated in the pLshC2c2 vector (R597A, H602A, R1278A, and H1283A) with protospacer 1. Images from plaque assay testing these HEPN mutant loci show similar plaque formation to the non-targeting locus and is significantly higher than the WtC2c2 locus. Phage dilutions were spotted on bacteria plates at decreasing numbers of plaque forming units (PFU). Spacer targets are shown above images; biological replicates are labeled BR1, BR2, or BR3. Non-targeting control is the native LshC2c2 locus.

Figure S14

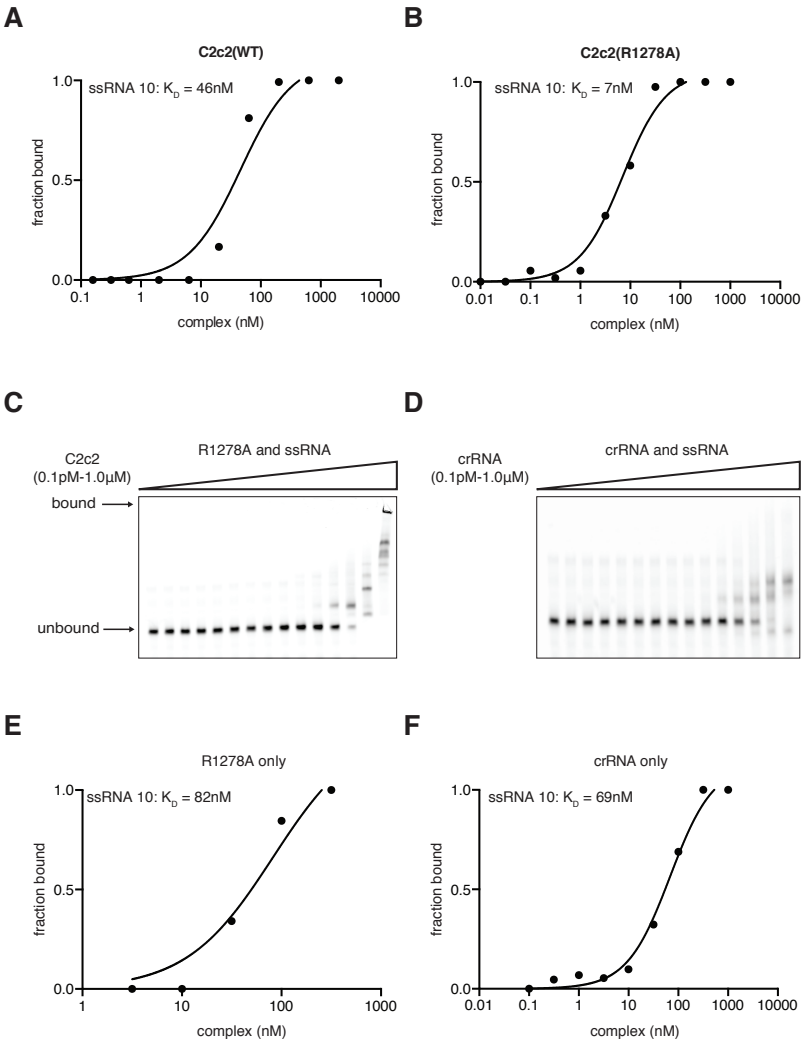

Fig. S14: Quantitation of LshC2c2 binding

(A) Calculation of binding affinity for wildtype LshC2c2-crRNA complex and on-target ssRNA. Fraction of protein bound was quantified by densitometry from Fig. 4D and K_D was calculated by fitting to binding isotherm. (B) Calculation of binding affinity for HEPN mutant R1278A LshC2c2-crRNA complex and on-target ssRNA. Fraction of protein bound was quantified by densitometry from Fig. 4E and K_D was calculated by fitting to binding isotherm. (C) Electrophoretic mobility shift assay with HEPN mutant R1278A LshC2c2 against on-target

ssRNA in the absence of crRNA. EDTA is supplemented to reaction condition. (D) Electrophoretic mobility shift assay crRNA against on-target ssRNA. EDTA is supplemented to reaction condition. (E) Calculation of binding affinity for HEPN mutant R1278A LshC2c2 and on-target ssRNA in the absence of crRNA. Fraction of protein bound was quantified by densitometry from Fig. S12C and K_D was calculated by fitting to binding isotherm. (F) Calculation of binding affinity for crRNA and on-target ssRNA. Fraction of crRNA bound was quantified by densitometry from Fig. S12D and K_D was calculated by fitting to binding isotherm.

Figure S15

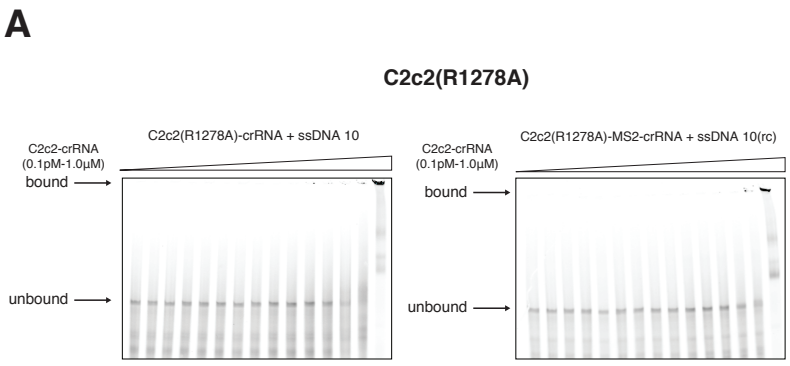

Fig. S15. LshC2c2-crRNA complex has little binding affinity for ssDNA targets.

Electrophoretic mobility shift assay with HEPN mutant R1278A LshC2c2 against on-target ssDNA and non-complementary ssDNA (reverse complement). EDTA is supplemented to reaction condition.

Figure S16

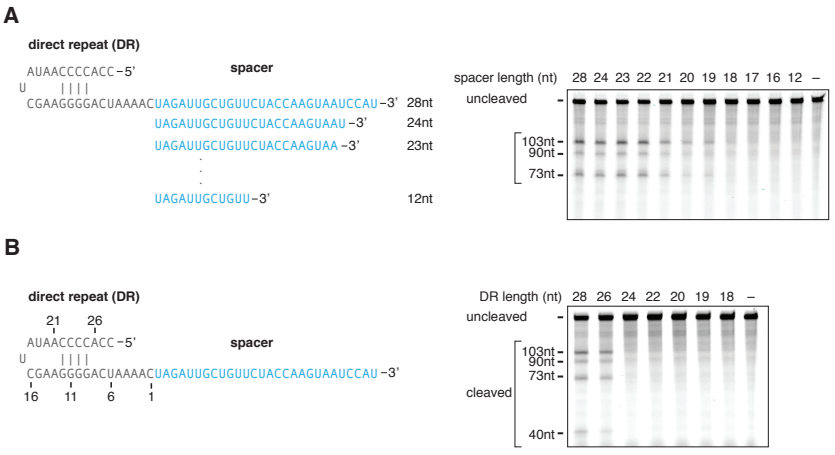

Fig. S16. Spacer and direct repeat lengths affect the RNA-guided RNase activity of LshC2c2.

(A) Denaturing gel showing crRNA-guided cleavage of ssRNA 1 as a function of spacer length after 3 hours of incubation. Reported band lengths are matched from RNA sequencing. (B) Denaturing gel showing crRNA-guided cleavage of ssRNA 1 as a function of the direct repeat length after 3 hours of incubation. Reported band lengths are matched from RNA sequencing.

Figure S17

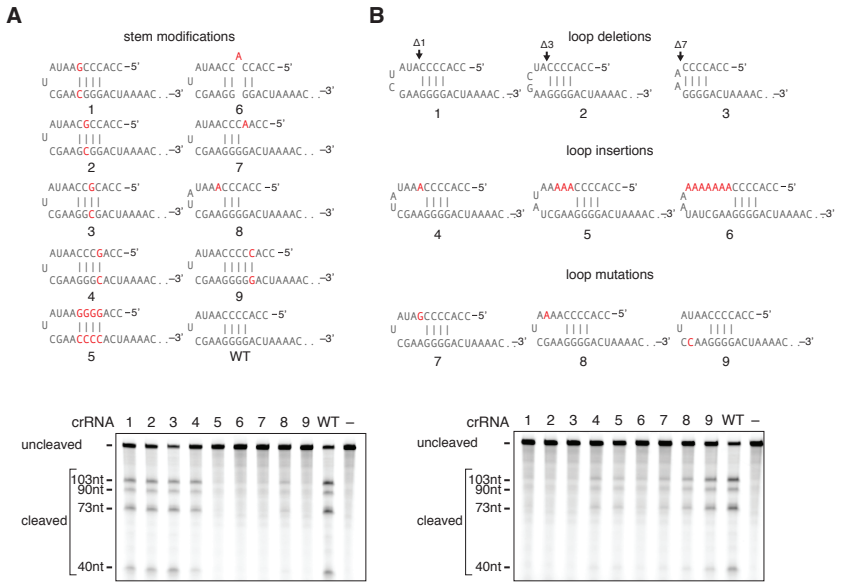

Fig. S17. RNA-guided RNase activity of LshC2c2 is dependent on direct repeat structure and sequence.

(A) Schematic showing modifications to the crRNA direct repeat stem (top). Altered bases are shown in red. Denaturing gel showing crRNA-guided cleavage of ssRNA 1 by each modified crRNA after 3 hours of incubation (bottom). Reported band lengths are matched from RNA sequencing. (B) Schematic showing modifications to the loop region of the crRNA direct repeat (top). Altered bases are shown in red and deletion lengths are indicated by arrows. Denaturing gel showing crRNA-guided cleavage of ssRNA 1 by each modified crRNA after 3 hours of incubation (bottom). Reported band lengths are matched from RNA sequencing.

Figure S18

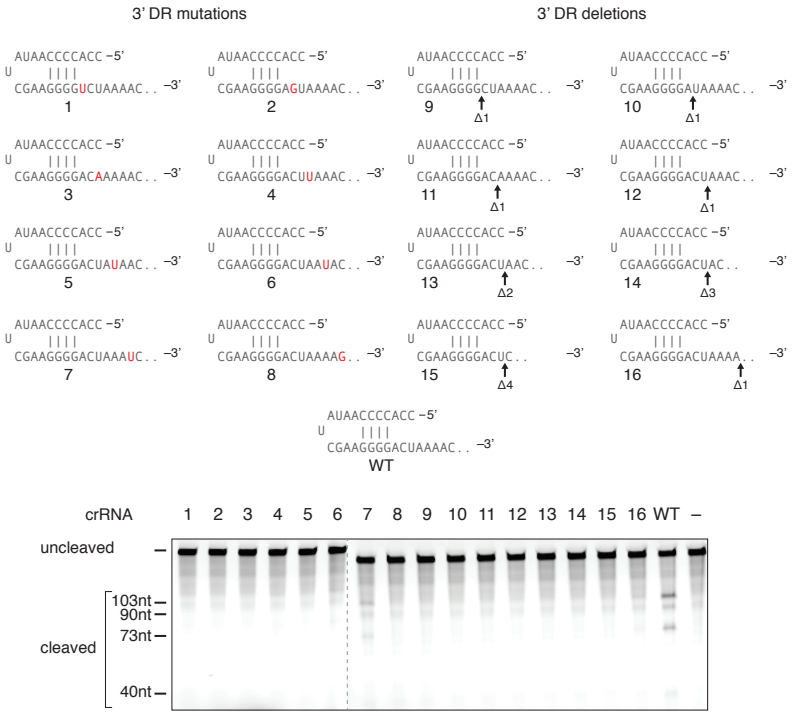

Fig. S18. The effect of 3' modifications to the crRNA DR.

Schematic shows the modifications made to the 3' end of the DR: single mutations *(top-left)* or deletions *(top-right)*. Altered bases are shown in red and deletion lengths are indicated by arrows. Denaturing gel depicting LshC2c2 cleavage activity by each modified crRNA after 3 hours of incubation *(bottom)*. Reported band lengths are matched from RNA sequencing.

Figure S19

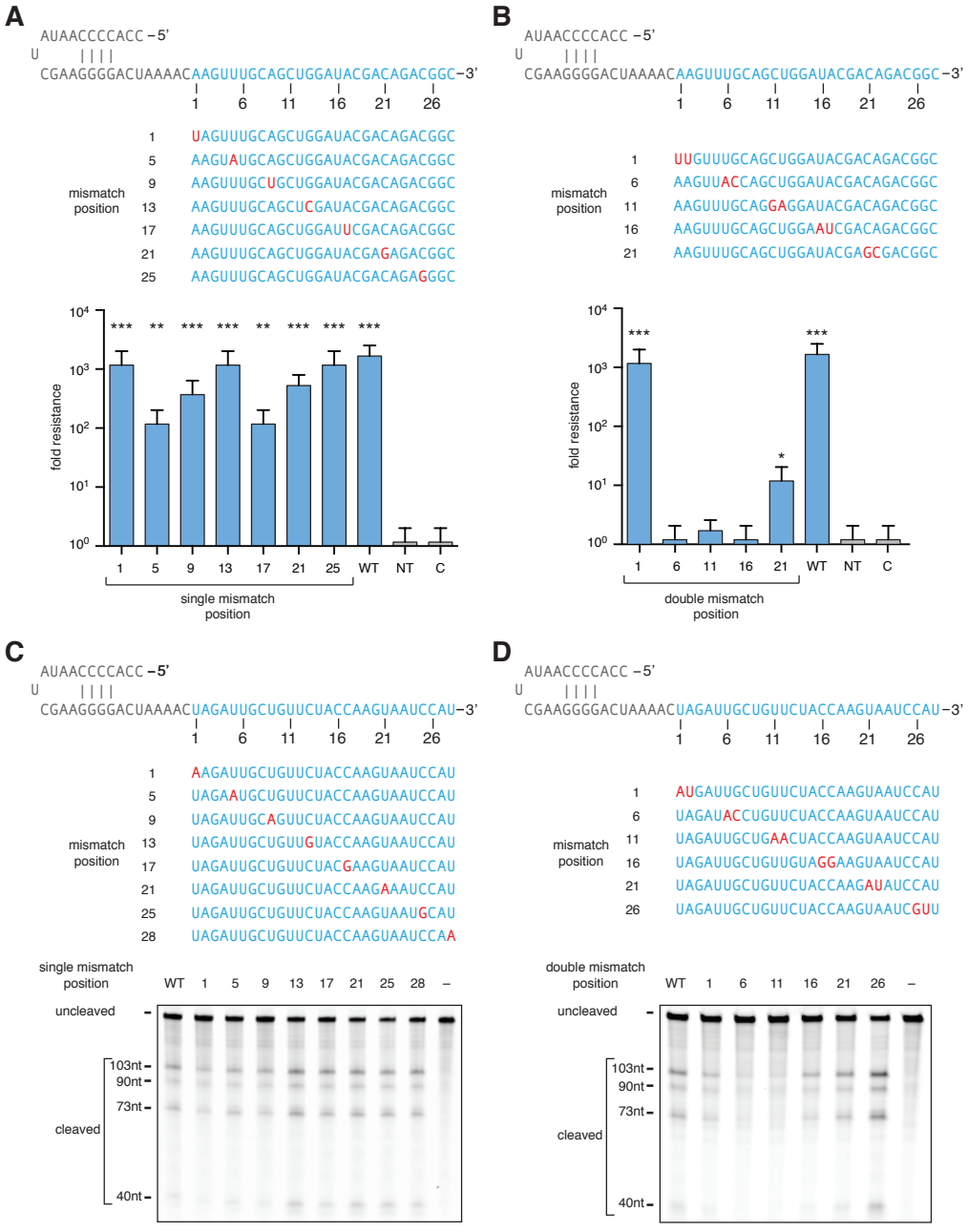

Fig. S19. Effect of RNA target-crRNA mismatches on LshC2c2 RNase activity.

(A) Quantification of MS2 plaque assays testing single mismatches at various positions in the spacer. Single mismatches have minimal effect on phage interference. Locations and identity of mismatches are shown in red. . (n=3 biological replicates. **, $p < 0.01$; ***, $p < 0.001$ compared to pACYC184 by t-test. Bars represent mean ± s.e.m). (B) Quantification of MS2 plaque assays

testing double mismatches at various positions in the spacer. Consecutive double mismatches in the middle of the spacer eliminate phage interference. Locations and identity of mismatches are shown in red. (n=3 biological replicates. ***, $p < 0.001$ compared to pACYC184 by t-test. Bars represent mean ± s.e.m). (C) Schematic showing the position and identity of single mismatches (red) in the crRNA spacer (top). Denaturing gel showing cleavage of ssRNA 1 guided by crRNAs with single mismatches in the spacer after 3 hours of incubation (bottom). Reported band lengths are matched from RNA sequencing. (D) Schematic showing the position and identity of pairs of mismatches (red) in the crRNA spacer (top). Denaturing gel showing cleavage of ssRNA 1 guided by crRNAs with pairs of mismatches in the spacer after 3 hours of incubation (bottom). Reported band lengths are matched from RNA sequencing.

Figure S20

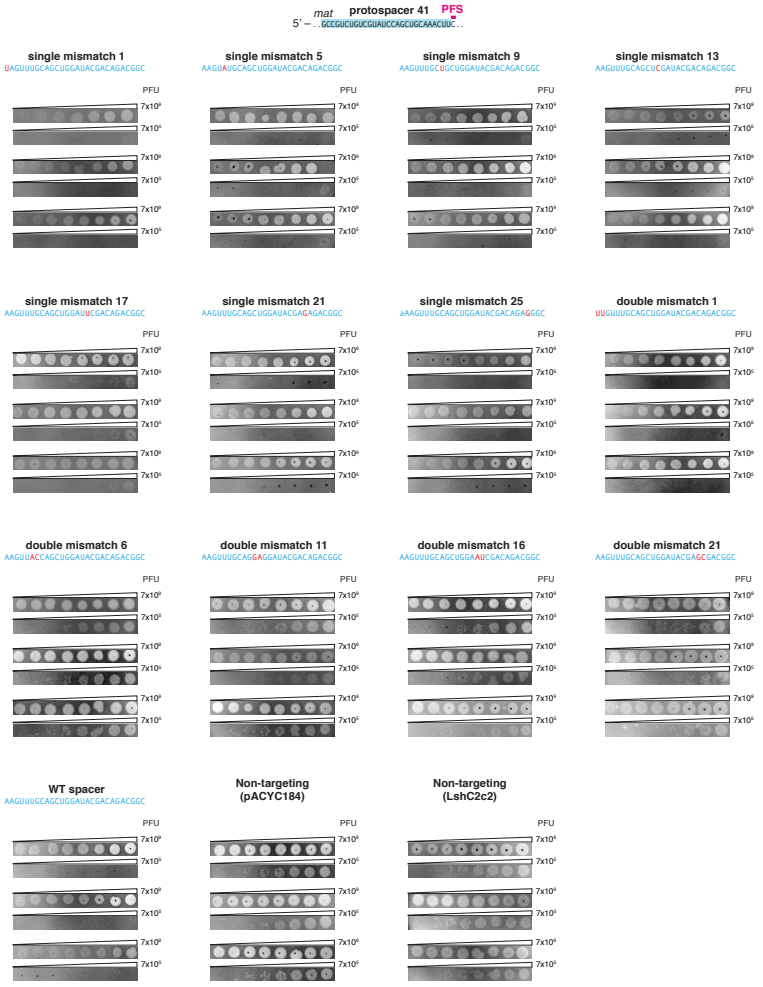

Fig. S20: MS2 restriction assay testing the effect of single and double mismatches on LshC2c2 activity.

pLshC2c2 with protospacer 41 was modified to have a series of single mismatches and consecutive double mismatches as shown. Images from plaque assay testing these mismatched spacers reveals reduced plaque formation for the single-mismatch spacers on-par with the fully complementary spacer. The double mismatch spacers show increased plaque formation for a seed region in the middle of spacer sequence. Phage dilutions were spotted on bacteria plates at decreasing numbers of plaque forming units (PFU). Spacer targets are shown above images;

biological replicates are labeled BR1, BR2, or BR3. Non-targeting control is the native LshC2c2 locus.

Figure S21

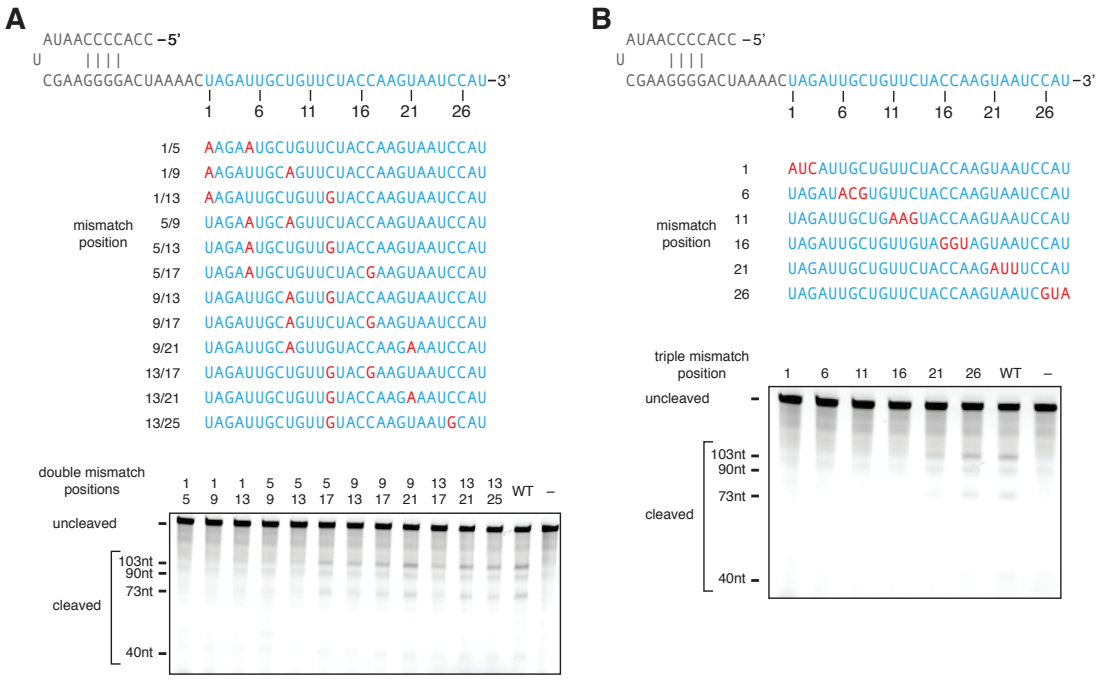

Fig. S21. The effect of triple mismatches on LshC2c2-crRNA cleavage activity.

(A) Schematic showing the position and identity of non-consecutive triple mismatches (red) in the crRNA spacer (top). Denaturing gel depicting LshC2c2 cleavage activity with crRNAs bearing triple non-consecutive mismatches between the spacer and ssRNA target region after 3 hours of incubation (bottom). Reported band lengths are matched from RNA sequencing. (B) Schematic showing the position and identity of consecutive triple mismatches (red) in the crRNA spacer (top). Denaturing gel depicting LshC2c2 cleavage activity with crRNAs bearing triple consecutive mismatches between the spacer and ssRNA target region after 3 hours of incubation (bottom). Reported band lengths are matched from RNA sequencing.

Figure S22

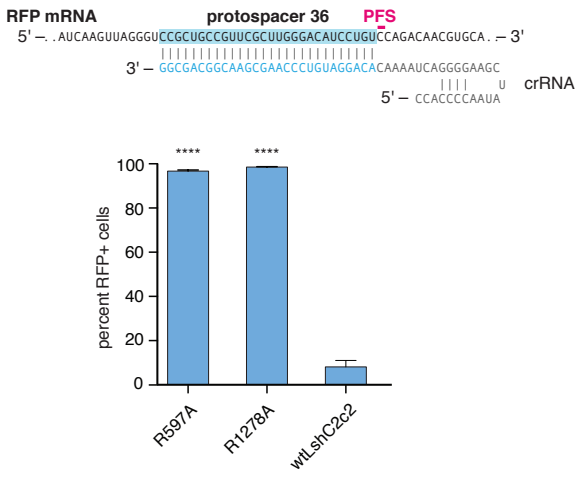

Fig. S22: HEPN mutant LshC2c2 are tested for RFP mRNA targeting activity.

The pLshC2c2 vector with protospacer 36 was modified to have the single HEPN mutants R597A and R1278A (one in each of the HEPN domains). These mutations resulted in little detectable RFP knockdown as measured by flow cytometry on the *E. coli*. (n=3 biological replicates. ***, $p < 0.001$ compared to wtLshC2c2 by t-test. Bars represent mean ± s.e.m)

Figure S23

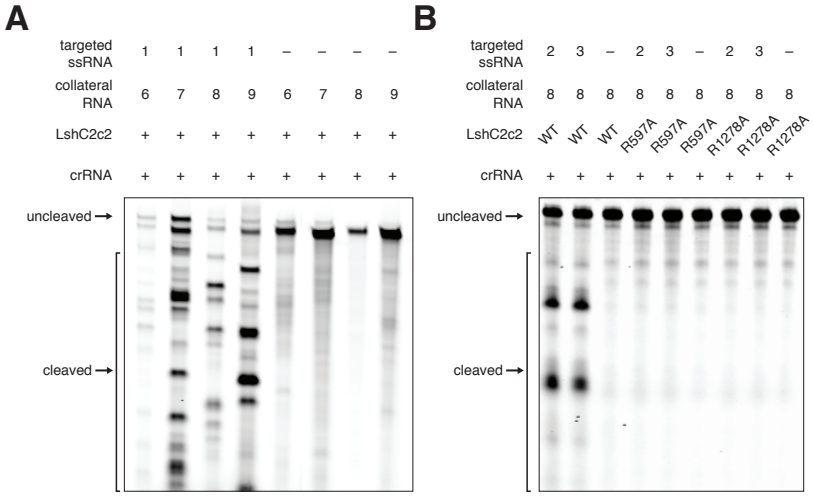

Fig. S23: Biochemical characterization of the collateral cleavage effect.

(A) LshCc2 is incubated for 3 hours with a crRNA targeting protospacer 14 with and without unlabeled ssRNA target 1 (contains protospacer 14). When LshC2c2 is in the presence of target 1, significant cleavage activity is observed for 5' fluorescently labeled non-complementary targets 6-9. (B) HEPN mutant collateral activity is compared to WT C2c2. The proteins are incubated for 3 hours with crRNA complementary to protospacer 14 and with and without unlabeled homopolymer targets 2 or 3 (both containing protospacer 14). The collateral effect is no longer observed with the HEPN mutant proteins on the 3' fluorescently labeled non-complementary target 8.

Figure S24

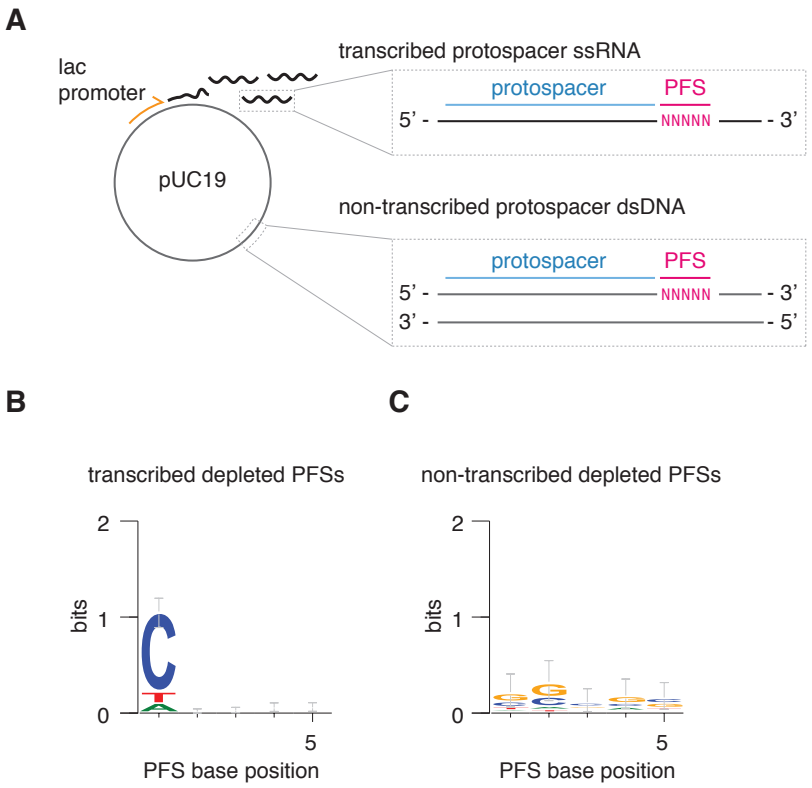

Fig. S24. *In vivo* collateral effect reveals a 3' H PFS with a PFS screen in a transcribed region.

(A) Schematic for a transcribed and non-transcribed PFS screen. (B) 3' PFS motif for a PFS screen designed in a transcribed plasmid region. (C) No PFS is observed for a PFS screen in a non-transcribed region.

Table S1. Number of top enriched crRNA sequences in all conditions of the MS2 screen.

Condition	# of targeting crRNAs with $\log_2$ normalized crRNA count > 1.25 (normalized to no phage condition)
Phage 10^{-1} dilution replicate 1	617
Phage 10^{-1} dilution replicate 2	630
Phage 10^{-1} dilution replicate 3	703
Phage 10^{-3} dilution replicate 1	508
Phage 10^{-3} dilution replicate 2	524
Phage 10^{-3} dilution replicate 3	436
Phage 10^{-5} dilution replicate 1	452
Phage 10^{-5} dilution replicate 2	515
Phage 10^{-5} dilution replicate 3	367

Table S2. crRNA sequences used for *in vitro* experiments.

Name	Sequence	1st Fig.
crRNA 14	CCACCCCAAUAUCGAAGGGGACUAAAACUAGAUUGCUGUUCUACCAAGUAAUCCAU	2B
crRNA 15	CCACCCCAAUAUCGAAGGGGACUAAAACUUUCUAGAGGAUCCCCGGGUACCGAGCU	2D
crRNA 16	CCACCCCAAUAUCGAAGGGGACUAAAACAGUAAUCCAUAUUUCUAGAGGAUCCCCG	2D
crRNA 17	CCACCCCAAUAUCGAAGGGGACUAAAACUAGAUUGCUGUUCUACCAAGUAAUCCAU	2D
crRNA 18	CCACCCCAAUAUCGAAGGGGACUAAAACCAUGCCUGCAGGUCGAGUAGAUUGCUGU	2D
crRNA 19	CCACCCCAAUsAUCGAAGGGGACUAAAACGCAUGCCUGCAGGUCGAGUAGAUUGCUG	2D
crRNA 20	CCACCCCAAUAUCGAAGGGGACUAAAACAAGCUUGCAUGCCUGCAGGUCGAGUAGA	2D
crRNA 21	CCACCCCAAUAUCGAAGGGGACUAAAACCGCCAAGCUUGCAUGCCUGCAGGUCGAG	2D
crRNA 22	CCACCCCAAUAUCGAAGGGGACUAAAACGAUUACGCCAAGCUUGCAUGCCUGCAGG	2D
crRNA 23	CCACCCCAAUAUCGAAGGGGACUAAAACUGAUUACGCCAAGCUUGCAUGCCUGCAG	2D
crRNA 24	CCACCCCAAUAUCGAAGGGGACUAAAACAUGACCAUGAUUACGCCAAGCUUGCAUG	2D
crRNA 25	CCACCCCAAUAUCGAAGGGGACUAAAACUAUGACCAUGAUUACGCCAAGCUUGCAU	2D
crRNA 26	CCACCCCAAUAUCGAAGGGGACUAAAACAGCUAUGACCAUGAUUACGCCAAGCUUG	2D
crRNA 27	CCACCCCAAUAUCGAAGGGGACUAAAACGAAACAGCUAUGACCAUGAUUACGCCAA	2D
crRNA 28	CCACCCCAAUAUCGAAGGGGACUAAAACACAGGAAACAGCUAUGACCAUGAUUACG	2D
crRNA 29	CCACCCCAAUAUCGAAGGGGACUAAAACAACACAGGAAACAGCUAUGACCAUGAUU	2D
crRNA 30	CCACCCCAAUAUCGAAGGGGACUAAAACAAACACAGGAAACAGCUAUGACCAUGAU	2D
crRNA 31	CCACCCCAAUAUCGAAGGGGACUAAAACAUAAACACAGGAAACAGCUAUGACCAUG	2D
crRNA 32	CCACCCCAAUAUCGAAGGGGACUAAAACGGAUAAACACAGGAAACAGCUAUGACCA	2D
crRNA 33	CCACCCCAAUAUCGAAGGGGACUAAAACAGCGGAUAAACACAGGAAACAGCUAUGA	2D
crRNA 34	CCACCCCAAUAUCGAAGGGGACUAAAACGAGCGGAUAAACACAGGAAACAGCUAUG	2D
Lsh_crRNA_DR_28	CCACCCCAAUAUCGAAGGGGACUAAAACUAGAUUGCUGUUCUACCAAGUAAUCCAU	S16B
Lsh_crRNA_DR_26	ACCCCAAUAUCGAAGGGGACUAAAACUAGAUUGCUGUUCUACCAAGUAAUCCAU	S16B
Lsh_crRNA_DR_24	CCCAAUAUCGAAGGGGACUAAAACUAGAUUGCUGUUCUACCAAGUAAUCCAU	S16B
Lsh_crRNA_DR_22	CAAUAUCGAAGGGGACUAAAACUAGAUUGCUGUUCUACCAAGUAAUCCAU	S16B
Lsh_crRNA_DR_20	AUAUCGAAGGGGACUAAAACUAGAUUGCUGUUCUACCAAGUAAUCCAU	S16B
Lsh_crRNA_DR_19	UAUCGAAGGGGACUAAAACUAGAUUGCUGUUCUACCAAGUAAUCCAU	S16B
Lsh_crRNA_DR_18	AUCGAAGGGGACUAAAACUAGAUUGCUGUUCUACCAAGUAAUCCAU	S16B
Lsh_crRNA_24	CCACCCCAAUAUCGAAGGGGACUAAAACUAGAUUGCUGUUCUACCAAGUAAU	S16A
Lsh_crRNA_23	CCACCCCAAUAUCGAAGGGGACUAAAACUAGAUUGCUGUUCUACCAAGUAA	S16A
Lsh_crRNA_22	CCACCCCAAUAUCGAAGGGGACUAAAACUAGAUUGCUGUUCUACCAAGUA	S16A
Lsh_crRNA_21	CCACCCCAAUAUCGAAGGGGACUAAAACUAGAUUGCUGUUCUACCAAGU	S16A

Lsh_crRNA_20	CCACCCCAAUAUCGAAGGGGACUAAAACUAGAUUGCUGUUCUACCAAG	S16A
Lsh_crRNA_19	CCACCCCAAUAUCGAAGGGGACUAAAACUAGAUUGCUGUUCUACCAA	S16A
Lsh_crRNA_18	CCACCCCAAUAUCGAAGGGGACUAAAACUAGAUUGCUGUUCUACCA	S16A
Lsh_crRNA_17	CCACCCCAAUAUCGAAGGGGACUAAAACUAGAUUGCUGUUCUACC	S16A
Lsh_crRNA_16	CCACCCCAAUAUCGAAGGGGACUAAAACUAGAUUGCUGUUCUAC	S16A
Lsh_crRNA_12	CCACCCCAAUAUCGAAGGGGACUAAAACUAGAUUGCUGUU	S16A
Lsh_stem_1	CCACCCGAAUAUCGAACGGGACUAAAACUAGAUUGCUGUUCUACCAAGUAAUCCAU	S17A
Lsh_stem_2	CCACCGCAAUAUCGAAGCGGACUAAAACUAGAUUGCUGUUCUACCAAGUAAUCCAU	S17A
Lsh_stem_3	CCACGCCAAUAUCGAAGGCGACUAAAACUAGAUUGCUGUUCUACCAAGUAAUCCAU	S17A
Lsh_stem_4	CCAGCCCAAUAUCGAAGGGCACUAAAACUAGAUUGCUGUUCUACCAAGUAAUCCAU	S17A
Lsh_stem_5	CCAGGGGGAAUAUCGAACCCCACUAAAACUAGAUUGCUGUUCUACCAAGUAAUCCAU	S17A
Lsh_stem_6	CCACCACCAAUAUCGAAGGGGACUAAAACUAGAUUGCUGUUCUACCAAGUAAUCCAU	S17A
Lsh_stem_7	CCAACCCAAUAUCGAAGGGGACUAAAACUAGAUUGCUGUUCUACCAAGUAAUCCAU	S17A
Lsh_stem_8	CCACCCAAAUAUCGAAGGGGACUAAAACUAGAUUGCUGUUCUACCAAGUAAUCCAU	S17A
Lsh_stem_9	CCACCCCCAAUAUCGAAGGGGGACUAAAACUAGAUUGCUGUUCUACCAAGUAAUCCAU	S17A
Lsh_loop_1	CCACCCCAUAUCGAAGGGGACUAAAACUAGAUUGCUGUUCUACCAAGUAAUCCAU	S17B
Lsh_loop_2	CCACCCCAUCGAAGGGGACUAAAACUAGAUUGCUGUUCUACCAAGUAAUCCAU	S17B
Lsh_loop_3	CCACCCCAAGGGGACUAAAACUAGAUUGCUGUUCUACCAAGUAAUCCAU	S17B
Lsh_loop_4	CCACCCCAAAUAUCGAAGGGGACUAAAACUAGAUUGCUGUUCUACCAAGUAAUCCAU	S17B
Lsh_loop_5	CCACCCCAAAAAUAUCGAAGGGGACUAAAACUAGAUUGCUGUUCUACCAAGUAAUCCAU	S17B
Lsh_loop_6	CCACCCCAAAAAAAAAUAUCGAAGGGGACUAAAACUAGAUUGCUGUUCUACCAAGUAAUCCAU	S17B
Lsh_loop_7	CCACCCCGAUAUCGAAGGGGACUAAAACUAGAUUGCUGUUCUACCAAGUAAUCCAU	S17B
Lsh_loop_8	CCACCCCAAAAUCGAAGGGGACUAAAACUAGAUUGCUGUUCUACCAAGUAAUCCAU	S17B
Lsh_loop_9	CCACCCCAAUAUCCAAGGGGACUAAAACUAGAUUGCUGUUCUACCAAGUAAUCCAU	S17B
Lsh_crRNA_flip_8	CCACCCCAAUAUCGAAGGGGUCUAAAACUAGAUUGCUGUUCUACCAAGUAAUCCAU	S18
Lsh_crRNA_flip_7	CCACCCCAAUAUCGAAGGGGAGUAAAACUAGAUUGCUGUUCUACCAAGUAAUCCAU	S18
Lsh_crRNA_flip_6	CCACCCCAAUAUCGAAGGGGACAAAAACUAGAUUGCUGUUCUACCAAGUAAUCCAU	S18
Lsh_crRNA_flip_5	CCACCCCAAUAUCGAAGGGGACUUAAACUAGAUUGCUGUUCUACCAAGUAAUCCAU	S18
Lsh_crRNA_flip_4	CCACCCCAAUAUCGAAGGGGACUAUAACUAGAUUGCUGUUCUACCAAGUAAUCCAU	S18
Lsh_crRNA_flip_3	CCACCCCAAUAUCGAAGGGGACUAAUACUAGAUUGCUGUUCUACCAAGUAAUCCAU	S18
Lsh_crRNA_flip_2	CCACCCCAAUAUCGAAGGGGACUAAAUCUAGAUUGCUGUUCUACCAAGUAAUCCAU	S18
Lsh_crRNA_flip_1	CCACCCCAAUAUCGAAGGGGACUAAAAGUAGAUUGCUGUUCUACCAAGUAAUCCAU	S18
Lsh_crRNA_delete_8	CCACCCCAAUAUCGAAGGGGCUAAAACUAGAUUGCUGUUCUACCAAGUAAUCCAU	S18

Lsh_crRNA_delete_7	CCACCCCAAUAUCGAAGGGGAUAAAACUAGAUUGCUGUUCUACCAAGUAAUCCAU	S18
Lsh_crRNA_delete_6	CCACCCCAAUAUCGAAGGGGACAAAACUAGAUUGCUGUUCUACCAAGUAAUCCAU	S18
Lsh_crRNA_delete_5	CCACCCCAAUAUCGAAGGGGACUAAACUAGAUUGCUGUUCUACCAAGUAAUCCAU	S18
Lsh_crRNA_delete_4	CCACCCCAAUAUCGAAGGGGACUAACUAGAUUGCUGUUCUACCAAGUAAUCCAU	S18
Lsh_crRNA_delete_3	CCACCCCAAUAUCGAAGGGGACUACUAGAUUGCUGUUCUACCAAGUAAUCCAU	S18
Lsh_crRNA_delete_2	CCACCCCAAUAUCGAAGGGGACUCUAGAUUGCUGUUCUACCAAGUAAUCCAU	S18
Lsh_crRNA_delete_1	CCACCCCAAUAUCGAAGGGGACUAAAAUAGAUUGCUGUUCUACCAAGUAAUCCAU	S18
Lsh_single_mismatch_pos1	CCACCCCAAUAUCGAAGGGGACUAAAACAAGAUUGCUGUUCUACCAAGUAAUCCAU	S19C
Lsh_single_mismatch_pos5	CCACCCCAAUAUCGAAGGGGACUAAAACUAGAAUGCUGUUCUACCAAGUAAUCCAU	S19C
Lsh_single_mismatch_pos9	CCACCCCAAUAUCGAAGGGGACUAAAACUAGAUUGCAGUUCUACCAAGUAAUCCAU	S19C
Lsh_single_mismatch_pos13	CCACCCCAAUAUCGAAGGGGACUAAAACUAGAUUGCUGUUGUACCAAGUAAUCCAU	S19C
Lsh_single_mismatch_pos17	CCACCCCAAUAUCGAAGGGGACUAAAACUAGAUUGCUGUUCUACGAAGUAAUCCAU	S19C
Lsh_single_mismatch_pos21	CCACCCCAAUAUCGAAGGGGACUAAAACUAGAUUGCUGUUCUACCAAGAAAUCCAU	S19C
Lsh_single_mismatch_pos25	CCACCCCAAUAUCGAAGGGGACUAAAACUAGAUUGCUGUUCUACCAAGUAAUGCAU	S19C
Lsh_single_mismatch_pos28	CCACCCCAAUAUCGAAGGGGACUAAAACUAGAUUGCUGUUCUACCAAGUAAUCCAA	S19C
Lsh_double_mismatch_pos1	CCACCCCAAUAUCGAAGGGGACUAAAACAUGAUUGCUGUUCUACCAAGUAAUCCAU	S19D
Lsh_double_mismatch_pos6	CCACCCCAAUAUCGAAGGGGACUAAAACUAGAUACCUGUUCUACCAAGUAAUCCAU	S19D
Lsh_double_mismatch_pos11	CCACCCCAAUAUCGAAGGGGACUAAAACUAGAUUGCUGAACUACCAAGUAAUCCAU	S19D
Lsh_double_mismatch_pos16	CCACCCCAAUAUCGAAGGGGACUAAAACUAGAUUGCUGUUCUAGGAAGUAAUCCAU	S19D
Lsh_double_mismatch_pos21	CCACCCCAAUAUCGAAGGGGACUAAAACUAGAUUGCUGUUCUACCAAGAUAUCCAU	S19D
Lsh_double_mismatch_pos26	CCACCCCAAUAUCGAAGGGGACUAAAACUAGAUUGCUGUUCUACCAAGUAAUCGUU	S19D
Lsh_crRNA_MM_2_1_5	CCACCCCAAUAUCGAAGGGGACUAAAACAAGAAUGCUGUUCUACCAAGUAAUCCAU	S21A
Lsh_crRNA_MM_2_1_9	CCACCCCAAUAUCGAAGGGGACUAAAACAAGAUUGCAGUUCUACCAAGUAAUCCAU	S21A

Lsh_crRNA_MM_2_1_13	CCACCCCAAUAUCGAAGGGGACUAAAACAAGAUUGCUGUUGUACCAAGUAAUCCAU	S21A
Lsh_crRNA_MM_2_5_9	CCACCCCAAUAUCGAAGGGGACUAAAACUAGAAUGCAGUUCUACCAAGUAAUCCAU	S21A
Lsh_crRNA_MM_2_5_13	CCACCCCAAUAUCGAAGGGGACUAAAACUAGAAUGCUGUUGUACCAAGUAAUCCAU	S21A
Lsh_crRNA_MM_2_5_17	CCACCCCAAUAUCGAAGGGGACUAAAACUAGAAUGCUGUUCUACGAAGUAAUCCAU	S21A
Lsh_crRNA_MM_2_9_13	CCACCCCAAUAUCGAAGGGGACUAAAACUAGAUUGCAGUUGUACCAAGUAAUCCAU	S21A
Lsh_crRNA_MM_2_9_17	CCACCCCAAUAUCGAAGGGGACUAAAACUAGAUUGCAGUUCUACGAAGUAAUCCAU	S21A
Lsh_crRNA_MM_2_9_21	CCACCCCAAUAUCGAAGGGGACUAAAACUAGAUUGCAGUUCUACCAAGAAAUCCAU	S21A
Lsh_crRNA_MM_2_13_17	CCACCCCAAUAUCGAAGGGGACUAAAACUAGAUUGCUGUUGUACGAAGUAAUCCAU	S21A
Lsh_crRNA_MM_2_13_21	CCACCCCAAUAUCGAAGGGGACUAAAACUAGAUUGCUGUUGUACCAAGAAAUCCAU	S21A
Lsh_crRNA_MM_2_13_25	CCACCCCAAUAUCGAAGGGGACUAAAACUAGAUUGCUGUUGUACCAAGUAAUGCAU	S21A
Lsh_crRNA_MM_3_1	CCACCCCAAUAUCGAAGGGGACUAAAACAUCAUUGCUGUUCUACCAAGUAAUCCAU	S21B
Lsh_crRNA_MM_3_6	CCACCCCAAUAUCGAAGGGGACUAAAACUAGAUACGUGUUCUACCAAGUAAUCCAU	S21B
Lsh_crRNA_MM_3_11	CCACCCCAAUAUCGAAGGGGACUAAAACUAGAUUGCUGAAGUACCAAGUAAUCCAU	S21B
Lsh_crRNA_MM_3_16	CCACCCCAAUAUCGAAGGGGACUAAAACUAGAUUGCUGUUCUAGGUAGUAAUCCAU	S21B
Lsh_crRNA_MM_3_21	CCACCCCAAUAUCGAAGGGGACUAAAACUAGAUUGCUGUUCUACCAAGAUUUCCAU	S21B

Table S3. ssRNA targets used in this study.

Name	Target	1st Fig.
ssRNA 1 (C PFS)	GGCCAGUGAAUUCGAGCUCGGUACCCGGGGAUCCUCUAGAAAUAUGGAUUACUUGG UAGAACAGCAAUCUACUCGACCUGCAGGCAUGCAAGCUUGGCGUAAUCAUGGUCAU AGCUGUUUCCUGUGUUUAUCCGCUCACAAUUCCACACAACAUACGAGCCGGAAGCA UAAAG	2B
ssRNA 2	AAUAUGGAUUACUUGGUAGAACAGCAAUCUACAAAAAAAAAAAAAAAAAAAAGAAAA AAAAAAAAAAAAAAAGAAAAAAAAAAAAAAAAAAAGAAAAAAAAAAAAAAAAAAG AAAAAAAAAAAAAAAAAAAGAAAAAAAAAAAAAAAAAAG	S12
ssRNA 3	AAUAUGGAUUACUUGGUAGAACAGCAAUCUACUUUUUUUUUUUUUUUUUUUCUUUU UUUUUUUUUUUUUUUCUUUUUUUUUUUUUUUUUUUCUUUUUUUUUUUUUUUUUUC UUUUUUUUUUUUUUUUUUUCUUUUUUUUUUUUUUUUUUC	S12
ssRNA 4	GGGUAGGUGUUCCACAGGGUAGCCAGCAGCAUCCUGCGAUGCAAAUAUGGAUUACU UGGUAGAACAGCAAUCUAAUCCGGAACAUAAUGGUGCAGGGCGCUGACUUCCGCGU UUCCAGACUUUACGAAACACGGAAACCGAAGACCAUUCAUGUUGUUGCUGCCGGAA GCAUAAAG	3A
ssRNA 5	GGGCCCCUCCGUUCGCGUUUACGCGGACGGUGAGACUGAAGAUAAUAUGGAUUACU UGGUAGAACAGCAAUCUAAACUCAUUCUCUUUAAAAUAUCGUUCGAACUGGACUCC CGGUCGUUUUAACUCGACUGGGGCCAAAACGAAACAGUGGCACUACCCCGCCGGAA GCAUAAAG	3A
ssRNA 1 (G PFS)	GGCCAGUGAAUUCGAGCUCGGUACCCGGGGAUCCUCUAGAAAUAUGGAUUACUUGG UAGAACAGCAAUCUAGUCGACCUGCAGGCAUGCAAGCUUGGCGUAAUCAUGGUCAU AGCUGUUUCCUGUGUUUAUCCGCUCACAAUUCCACACAACAUACGAGCCGGAAGCA UAAAG	2C
ssRNA 1 (A PFS)	GGCCAGUGAAUUCGAGCUCGGUACCCGGGGAUCCUCUAGAAAUAUGGAUUACUUGG UAGAACAGCAAUCUAAUCGACCUGCAGGCAUGCAAGCUUGGCGUAAUCAUGGUCAU AGCUGUUUCCUGUGUUUAUCCGCUCACAAUUCCACACAACAUACGAGCCGGAAGCA UAAAG	2C
ssRNA 1 (U PFS)	GGCCAGUGAAUUCGAGCUCGGUACCCGGGGAUCCUCUAGAAAUAUGGAUUACUUGG UAGAACAGCAAUCUAUUCGACCUGCAGGCAUGCAAGCUUGGCGUAAUCAUGGUCAU AGCUGUUUCCUGUGUUUAUCCGCUCACAAUUCCACACAACAUACGAGCCGGAAGCA UAAAG	2C
ssRNA 6	ACCGAUCGUCGUUGUUUGGGCAAUGCACGUUCUCCAACGGUGCUCCUAUGGGGCAC AAGUUGCAGGAUGCAGCGCCUUACAAGAAGUUCGCUGAACAAGCAACCGUUACCCC CCGCGCUCUGAGAGCGGCUCUAUUGGUCCGAGACCAAUGUGCGCCGUGGAUCAGAC ACGCGGU	6B
ssRNA 7	ACUGUUGGUGGUGUAGAGCUUCCUGUAGCCGCAUGGCGUUCGUACUUAAAUAUGGA ACUAACCAUUCCAAUUUUCGCUACGAAUUCCGACUGCGAGCUUAUUGUUAAGGCAA UGCAAGGUCUCCUAAAAGAUGGAAACCCGAUUCCCUCAGCAAUCGCAGCAAACUCC GGCAUCU	6B
ssRNA 8	GGUAACAUGCUCGAGGGCCUUACGGCCCCCGUGGGAUGCUCCUACAUGUCAGGAAC AGUUACUGACGUAAUAACGGGUGAGUCCAUCAUAAGCGUUGACGCUCCCUACGGGU GGACUGUGGAGAGACAGGGCACUGCUAAGGCCCAAAUCUCAGCCAUGCAUCGAGGG GUACAAU	6B
ssRNA 9	UUCGUAAAACGUUCGUGUCCGGGCUCUUUCGCGAGAGCUGCGGCGCGCACUUUUAC CGUGGUGUCGAUGUCAAACCGUUUUACAUCAAGAAACCUGUUGACAAUCUCUUCGC CCUGAUGCUGAUAUUAAAUCGGCUACGGGGUUGGGGAGUUGUCGGAGGUAUGUCAG AUCCACG	6B
ssRNA 10	AUAGGCCAGUGAAUUCGAGCUCGAAUAUGGAUUACUUGGUAGAACAGCAAUCUACG CCGGAAGCAUAAAG	4D
ssRNA 10(rc)	CUUUAUGCUUCCGGCGUAGAUUGCUGUUCUACCAAGUAAUCCAUAUUCGAGCUCGA AUUCACUGGCCUAU	4D
ssDNA target	ctttatgcttccggctcgtatgttgtgtggaattgtgagcggataaacacaggaaa	S10D

	cagctatgaccatgattacgccaagcttgcatgcctgcaggtcgagaatatggatt acttggtagaacagcaatctatctagaggatccccgggtaccgagctcgaattcac tggccccctatagtgagtcgtattaatttc	
modified ssRNA 1 U40A	GGGGGCCAGUGAAUUCGAGCUCGGUACCCGGGGAUCCUCAAGAAAUAUGGAUUACU UGGUAGAACAGCAAUCUACUCGACCUGCAGGCAUGCAAGCUUGGCGUAAUCAUGGU CAUAGCUGUUUCCUGUGUUUAUCCGCUCACAAUUCCACACAACAUACGAGCCGGAA GCAUAAAG	3D
modified ssRNA 1 U73A	GGGGGCCAGUGAAUUCGAGCUCGGUACCCGGGGAUCCUCUAGAAAUAUGGAUUACU UGGUAGAACAGCAAUCAACUCGACCUGCAGGCAUGCAAGCUUGGCGUAAUCAUGGU CAUAGCUGUUUCCUGUGUUUAUCCGCUCACAAUUCCACACAACAUACGAGCCGGAA GCAUAAAG	3D
modified ssRNA 1 U90A	GGGGGCCAGUGAAUUCGAGCUCGGUACCCGGGGAUCCUCUAGAAAUAUGGAUUACU UGGUAGAACAGCAAUCUACUCGACCUGCAGGCAAGCAAGCUUGGCGUAAUCAUGGU CAUAGCUGUUUCCUGUGUUUAUCCGCUCACAAUUCCACACAACAUACGAGCCGGAA GCAUAAAG	3D
modified ssRNA 1 U103A	GGGGGCCAGUGAAUUCGAGCUCGGUACCCGGGGAUCCUCUAGAAAUAUGGAUUACU UGGUAGAACAGCAAUCUACUCGACCUGCAGGCAUGCAAGCUUGGCGAAAUCAUGGU CAUAGCUGUUUCCUGUGUUUAUCCGCUCACAAUUCCACACAACAUACGAGCCGGAA GCAUAAAG	3D
modified ssRNA 4 poly U	GGGUAGGUGUUCCACAGGGUAGCCAGCAGCAUCCUGCGAUGCAAAUAUGGAUUACU UGGUAGAACAGCAAUCUAAUCCGGAACAUAAUGGUGCAGGGCGCUGACUUCCGCGU UUGUUUUAAAUCAAACACGGAAACCGAAGACCAUUCAUGUUGUUGCUGCCGGAAGC AUAAAG	S12G
modified ssRNA 4 poly C	GGGUAGGUGUUCCACAGGGUAGCCAGCAGCAUCCUGCGAUGCAAAUAUGGAUUACU UGGUAGAACAGCAAUCUAAUCCGGAACAUAAUGGUGCAGGGCGCUGACUUCCGCGU UUGCCCCAAACCAAACACGGAAACCGAAGACCAUUCAUGUUGUUGCUGCCGGAAGC AUAAAG	S12G
modified ssRNA 4 poly G	GGGUAGGUGUUCCACAGGGUAGCCAGCAGCAUCCUGCGAUGCAAAUAUGGAUUACU UGGUAGAACAGCAAUCUAAUCCGGAACAUAAUGGUGCAGGGCGCUGACUUCCGCGU UUGGGGGAAAGCAAACACGGAAACCGAAGACCAUUCAUGUUGUUGCUGCCGGAAGC AUAAAG	S12G
modified ssRNA 4 poly A	GGGUAGGUGUUCCACAGGGUAGCCAGCAGCAUCCUGCGAUGCAAAUAUGGAUUACU UGGUAGAACAGCAAUCUAAUCCGGAACAUAAUGGUGCAGGGCGCUGACUUCCGCGU UUGAAAAAAAACAAACACGGAAACCGAAGACCAUUCAUGUUGUUGCUGCCGGAAGC AUAAAG	S12G

Table S4. Spacers used for *in vivo* experiments.

Name	Sequence	1st Fig.
spacer 1	GAAGUUUGCAGCUGGAUACGACAGACGG	1D
spacer 2	UGUCUGGAAGUUUGCAGCUGGAUACGAC	1D
spacer 3	AGCUGGAUACGACAGACGGCCAUCUAAC	1D
spacer 4	UACGUCGCGAUAUGUUGCACGUUGUCUG	1D
spacer 5	UACGGACGACCUUCACCUUCACCUUCGAUUU	5A
spacer 6	UCGUACGGACGACCUUCACCUUCACCUUCGA	5A
spacer 7	CGGUCUGGGUACCUUCGUACGGACGACCUUC	5A
spacer 8	GCGGUCUGGGUACCUUCGUACGGACGACCUU	5A
spacer 9	AGCGGUCUGGGUACCUUCGUACGGACGACCU	5A
spacer 10	AGUUCAUAACACGUUCCCAUUUGAAACCUUC	5A
spacer 11	UUAACUUUGUAGAUGAACUCACCGUCUUGCA	5A
spacer 12	UUUAACUUUGUAGAUGAACUCACCGUCUUGC	5A
spacer 13	GUUUAACUUUGUAGAUGAACUCACCGUCUUG	5A
spacer 35	AAGUUUGCAGCUGGAUACGACAGACGGC	4B
spacer 36	ACAGGAUGUCCCAAGCGAACGGCAGCGG	S22
spacer 37	GCUUGUUCAGCGAACUUCUUGUAAGGCG	S4A
spacer 38	UAAGCUCGCAGUCGGAAUUCGUAGCGAA	S4A
spacer 39	CGUCAACGCUUAUGAUGGACUCACCCGU	S4A
spacer 40	UCAACAGGUUUCUUGAUGUAAAACGGUU	S4A
spacer 41	AAGUUUGCAGCUGGAUACGACAGACGGC	S5
spacer 42	UUUGCAGCUGGAUACGACAGACGGCCAU	S5
spacer 43	CAGCUGGAUACGACAGACGGCCAUCUAA	S5
spacer 44	GUUGUCUGGAAGUUUGCAGCUGGAUACG	S5
spacer 45	GCGAUAUGUUGCACGUUGUCUGGAAGUU	S5
spacer 46	ACGUUGUCUGGAAGUUUGCAGCUGGAUA	S5
spacer 47	AUGUUGCACGUUGUCUGGAAGUUUGCAG	S5
spacer 48	UGCAGCUGGAUACGACAGACGGCCAUCU	S5
spacer 49	CUGGAAGUUUGCAGCUGGAUACGACAGA	S5
spacer 50	AGUUUGCAGCUGGAUACGACAGACGGCC	S5
spacer 51	GCUGGAUACGACAGACGGCCAUCUAACU	S5
spacer 52	GUUUGCAGCUGGAUACGACAGACGGCCA	S5
spacer_41_single_mismatch_pos1	UAGUUUGCAGCUGGAUACGACAGACGGC	S19A

spacer_41_single_mismatch_pos5	AAGUAUGCAGCUGGAUACGACAGACGGC	S19A
spacer_41_single_mismatch_pos9	AAGUUUGCUGCUGGAUACGACAGACGGC	S19A
spacer_41_single_mismatch_pos13	AAGUUUGCAGCUCGAUACGACAGACGGC	S19A
spacer_41_single_mismatch_pos17	AAGUUUGCAGCUGGAUUCGACAGACGGC	S19A
spacer_41_single_mismatch_pos21	AAGUUUGCAGCUGGAUACGAGAGACGGC	S19A
spacer_41_single_mismatch_pos25	AAGUUUGCAGCUGGAUACGACAGAGGGC	S19A
spacer_41_double_mismatch_pos1	UUGUUUGCAGCUGGAUACGACAGACGGC	S19B
spacer_41_double_mismatch_pos6	AAGUUACCAGCUGGAUACGACAGACGGC	S19B
spacer_41_double_mismatch_pos11	AAGUUUGCAGGAGGAUACGACAGACGGC	S19B
spacer_41_double_mismatch_pos16	AAGUUUGCAGCUGGAAUCGACAGACGGC	S19B
spacer_41_double_mismatch_pos21	AAGUUUGCAGCUGGAUACGAGUGACGGC	S19B

Table S5. Plasmid maps for experiments in this study.

Plasmid Name	Link to plasmid map in Benchling
huLshC2c2-MBP for bacterial expression	https://benchling.com/s/Jl1pExm8/edit
LshC2c2 locus into pACYC184	https://benchling.com/s/E8LxbHUl/edit
LshC2c2 locus into pACYC184 with BsaI sites for spacer cloning	https://benchling.com/s/nJshaXmE/edit
PFS library in Beta-lactamase gene Screening Plasmid	https://benchling.com/s/lPJ1cCwR/edit
transcribed PFS library	https://benchling.com/s/yE6mFoYb/edit
non-transcribed PFS library	https://benchling.com/s/JoOerzaE/edit
pRFP with constitutive expression	https://benchling.com/s/JJrHLrVZ/edit
pBR322 with tetR-inducible RFP	https://benchling.com/s/JmviNU13/edit

SUPPLEMENTARY REFERENCES

1. K. S. Makarova *et al*., An updated evolutionary classification of CRISPR-Cas systems. *Nat Rev Microbiol* **13**, 722-736 (2015).
2. K. S. Makarova *et al*., Evolution and classification of the CRISPR-Cas systems. *Nat Rev Microbiol* **9**, 467-477 (2011).
3. A. V. Wright, J. K. Nunez, J. A. Doudna, Biology and Applications of CRISPR Systems: Harnessing Nature's Toolbox for Genome Engineering. *Cell* **164**, 29-44 (2016).
4. L. A. Marraffini, CRISPR-Cas immunity in prokaryotes. *Nature* **526**, 55-61 (2015).
5. J. van der Oost, M. M. Jore, E. R. Westra, M. Lundgren, S. J. Brouns, CRISPR-based adaptive and heritable immunity in prokaryotes. *Trends Biochem Sci* **34**, 401-407 (2009).
6. S. J. Brouns *et al*., Small CRISPR RNAs guide antiviral defense in prokaryotes. *Science* **321**, 960-964 (2008).
7. C. R. Hale *et al*., RNA-guided RNA cleavage by a CRISPR RNA-Cas protein complex. *Cell* **139**, 945-956 (2009).
8. R. N. Jackson *et al*., Structural biology. Crystal structure of the CRISPR RNA-guided surveillance complex from Escherichia coli. *Science* **345**, 1473-1479 (2014).
9. L. A. Marraffini, E. J. Sontheimer, CRISPR interference limits horizontal gene transfer in staphylococci by targeting DNA. *Science* **322**, 1843-1845 (2008).
10. S. Mulepati, A. Heroux, S. Bailey, Structural biology. Crystal structure of a CRISPR RNA-guided surveillance complex bound to a ssDNA target. *Science* **345**, 1479-1484 (2014).
11. T. Sinkunas *et al*., In vitro reconstitution of Cascade-mediated CRISPR immunity in Streptococcus thermophilus. *EMBO J* **32**, 385-394 (2013).
12. G. Gasiunas, R. Barrangou, P. Horvath, V. Siksnys, Cas9-crRNA ribonucleoprotein complex mediates specific DNA cleavage for adaptive immunity in bacteria. *Proc Natl Acad Sci U S A* **109**, E2579-2586 (2012).
13. M. Jinek *et al*., A programmable dual-RNA-guided DNA endonuclease in adaptive bacterial immunity. *Science* **337**, 816-821 (2012).
14. E. Deltcheva *et al*., CRISPR RNA maturation by trans-encoded small RNA and host factor RNase III. *Nature* **471**, 602-607 (2011).
15. R. Sapranauskas *et al*., The Streptococcus thermophilus CRISPR/Cas system provides immunity in Escherichia coli. *Nucleic Acids Res* **39**, 9275-9282 (2011).
16. J. E. Garneau *et al*., The CRISPR/Cas bacterial immune system cleaves bacteriophage and plasmid DNA. *Nature* **468**, 67-71 (2010).
17. R. Barrangou *et al*., CRISPR provides acquired resistance against viruses in prokaryotes. *Science* **315**, 1709-1712 (2007).
18. B. Zetsche *et al*., Cpf1 is a single RNA-guided endonuclease of a class 2 CRISPR-Cas system. *Cell* **163**, 759-771 (2015).
19. S. Shmakov *et al*., Discovery and Functional Characterization of Diverse Class 2 CRISPR-Cas Systems. *Mol Cell* **60**, 385-397 (2015).
20. C. R. Hale *et al*., Essential features and rational design of CRISPR RNAs that function with the Cas RAMP module complex to cleave RNAs. *Mol Cell* **45**, 292-302 (2012).
21. W. Jiang, P. Samai, L. A. Marraffini, Degradation of Phage Transcripts by CRISPR-Associated RNases Enables Type III CRISPR-Cas Immunity. *Cell* **164**, 710-721 (2016).

22. P. Samai *et al*., Co-transcriptional DNA and RNA Cleavage during Type III CRISPR-Cas Immunity. *Cell* **161**, 1164-1174 (2015).
23. R. H. Staals *et al*., Structure and activity of the RNA-targeting Type III-B CRISPR-Cas complex of Thermus thermophilus. *Mol Cell* **52**, 135-145 (2013).
24. R. H. Staals *et al*., RNA targeting by the type III-A CRISPR-Cas Csm complex of Thermus thermophilus. *Mol Cell* **56**, 518-530 (2014).
25. G. Tamulaitis *et al*., Programmable RNA shredding by the type III-A CRISPR-Cas system of Streptococcus thermophilus. *Mol Cell* **56**, 506-517 (2014).
26. V. Anantharaman, K. S. Makarova, A. M. Burroughs, E. V. Koonin, L. Aravind, Comprehensive analysis of the HEPN superfamily: identification of novel roles in intra-genomic conflicts, defense, pathogenesis and RNA processing. *Biol Direct* **8**, 15 (2013).
27. O. Niewoehner, M. Jinek, Structural basis for the endoribonuclease activity of the type III-A CRISPR-associated protein Csm6. *RNA* **22**, 318-329 (2016).
28. N. F. Sheppard, C. V. Glover, 3rd, R. M. Terns, M. P. Terns, The CRISPR-associated Csx1 protein of Pyrococcus furiosus is an adenosine-specific endoribonuclease. *RNA* **22**, 216-224 (2016).
29. G. W. Goldberg, W. Jiang, D. Bikard, L. A. Marraffini, Conditional tolerance of temperate phages via transcription-dependent CRISPR-Cas targeting. *Nature* **514**, 633-637 (2014).
30. L. Deng, R. A. Garrett, S. A. Shah, X. Peng, Q. She, A novel interference mechanism by a type IIIB CRISPR-Cmr module in Sulfolobus. *Mol Microbiol* **87**, 1088-1099 (2013).
31. Y. K. Kim, Y. G. Kim, B. H. Oh, Crystal structure and nucleic acid-binding activity of the CRISPR-associated protein Csx1 of Pyrococcus furiosus. *Proteins* **81**, 261-270 (2013).
32. J. K. Nunez, A. S. Lee, A. Engelman, J. A. Doudna, Integrase-mediated spacer acquisition during CRISPR-Cas adaptive immunity. *Nature*, (2015).
33. R. Heler *et al*., Cas9 specifies functional viral targets during CRISPR-Cas adaptation. *Nature*, (2015).
34. J. K. Nunez *et al*., Cas1-Cas2 complex formation mediates spacer acquisition during CRISPR-Cas adaptive immunity. *Nature structural & molecular biology* **21**, 528-534 (2014).
35. C. Diez-Villasenor, N. M. Guzman, C. Almendros, J. Garcia-Martinez, F. J. Mojica, CRISPR-spacer integration reporter plasmids reveal distinct genuine acquisition specificities among CRISPR-Cas I-E variants of Escherichia coli. *RNA Biol* **10**, 792-802 (2013).
36. I. Yosef, M. G. Goren, U. Qimron, Proteins and DNA elements essential for the CRISPR adaptation process in Escherichia coli. *Nucleic Acids Res* **40**, 5569-5576 (2012).
37. K. A. Datsenko *et al*., Molecular memory of prior infections activates the CRISPR/Cas adaptive bacterial immunity system. *Nat Commun* **3**, 945 (2012).
38. L. A. Marraffini, E. J. Sontheimer, Self versus non-self discrimination during CRISPR RNA-directed immunity. *Nature* **463**, 568-571 (2010).
39. C. R. Hale, A. Cocozaki, H. Li, R. M. Terns, M. P. Terns, Target RNA capture and cleavage by the Cmr type III-B CRISPR-Cas effector complex. *Genes Dev* **28**, 2432-2443 (2014).
40. J. Zhang *et al*., Structure and mechanism of the CMR complex for CRISPR-mediated antiviral immunity. *Mol Cell* **45**, 303-313 (2012).

41. G. Kozlov *et al*., Structural Basis of Defects in the Sacsin HEPN Domain Responsible for Autosomal Recessive Spastic Ataxia of Charlevoix-Saguenay (ARSACS). *J Biol Chem* **286**, 20407-20412 (2011).
42. S. Kiani *et al*., Cas9 gRNA engineering for genome editing, activation and repression. *Nat Methods* **12**, 1051-1054 (2015).
43. S. Konermann *et al*., Genome-scale transcriptional activation by an engineered CRISPR-Cas9 complex. *Nature* **517**, 583-588 (2015).
44. J. E. Dahlman *et al*., Orthogonal gene knockout and activation with a catalytically active Cas9 nuclease. *Nat Biotechnol* **33**, 1159-1161 (2015).
45. K. S. Makarova, Y. I. Wolf, E. V. Koonin, Comprehensive comparative-genomic analysis of type 2 toxin-antitoxin systems and related mobile stress response systems in prokaryotes. *Biol Direct* **4**, 19 (2009).
46. F. Hayes, L. Van Melderen, Toxins-antitoxins: diversity, evolution and function. *Crit Rev Biochem Mol Biol* **46**, 386-408 (2011).
47. K. S. Makarova, V. Anantharaman, L. Aravind, E. V. Koonin, Live virus-free or die: coupling of antivirus immunity and programmed suicide or dormancy in prokaryotes. *Biol Direct* **7**, 40 (2012).
48. C. Benda *et al*., Structural model of a CRISPR RNA-silencing complex reveals the RNA-target cleavage activity in Cmr4. *Mol Cell* **56**, 43-54 (2014).
49. Z. Abil, H. Zhao, Engineering reprogrammable RNA-binding proteins for study and manipulation of the transcriptome. *Mol Biosyst* **11**, 2658-2665 (2015).
50. J. P. Mackay, J. Font, D. J. Segal, The prospects for designer single-stranded RNA-binding proteins. *Nature structural & molecular biology* **18**, 256-261 (2011).
51. A. Filipovska, O. Rackham, Designer RNA-binding proteins: New tools for manipulating the transcriptome. *RNA Biol* **8**, 978-983 (2011).
52. S. Silas *et al*., Direct CRISPR spacer acquisition from RNA by a natural reverse transcriptase-Cas1 fusion protein. *Science* **351**, aad4234 (2016).
53. H. Li, R. Durbin, Fast and accurate short read alignment with Burrows-Wheeler transform. *Bioinformatics* **25**, 1754-1760 (2009).
54. G. E. Crooks, G. Hon, J. M. Chandonia, S. E. Brenner, WebLogo: a sequence logo generator. *Genome research* **14**, 1188-1190 (2004).
55. A. Liberzon *et al*., The Molecular Signatures Database (MSigDB) hallmark gene set collection. *Cell Syst* **1**, 417-425 (2015).